AD-A039 061 PENNSYLVANIA STATE UNIV UNIVERSITY PARK DEPT OF AERO--ETC F/G 20/4
MEASUREMENTS OF MOLECULAR STRETCHING IN IRROTATIONAL FLOW BY LI--ETC(U)
NOV 76 G L DENNISON

UNCLASSIFIED NL

| OF |
AD
A039061

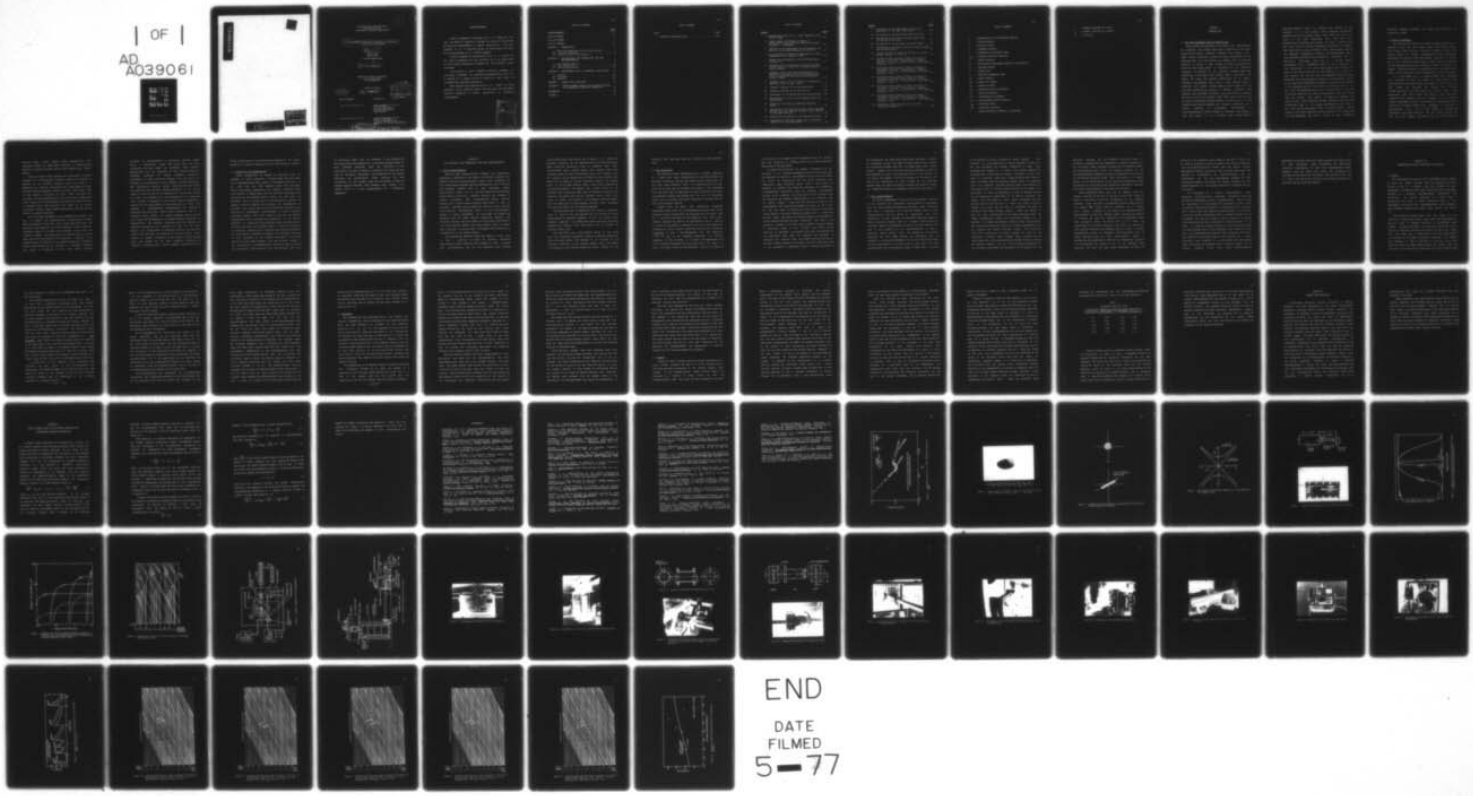

END

DATE
FILMED
5-77

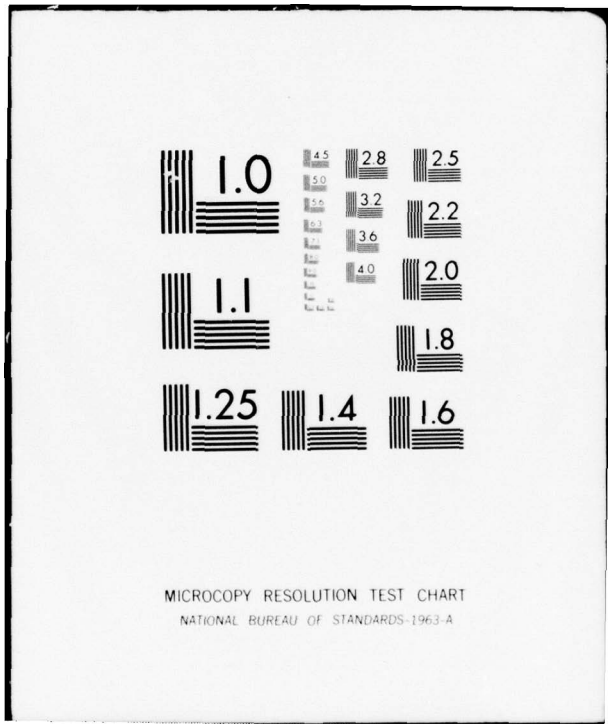
1.0
1.1
1.25
1.4
1.6
1.8
2.0
2.2
2.5
2.8
3.2
3.6
4.0
4.5
5.0
5.6
6.3
MICROCOPY RESOLUTION TEST CHART
NATIONAL BUREAU OF STANDARDS-1963-A

The Pennsylvania State University
The Graduate School
Department of Aerospace Engineering

Measurements of Molecular Stretching in Irrotational Flow by Light Scattering.

A Thesis in

Aerospace Engineering

by

Gary Lee Dennison

Submitted in Partial Fulfillment
of the Requirements
for the Degree of

Master of Science

November 1976

Date of Approval:

Signatories:

_____

_____
John L. Lumley,
Evan Pugh Professor of
Aerospace Engineering
Thesis Advisor

_____

_____
Barnes W. McCormick,
Professor and Head of the
Department of Aerospace Engineering

ACKNOWLEDGMENTS

I wish to express my gratitude to Dr. J. L. Lumley for his time and effort in guiding me through the course of this study. His help and encouragement is deeply appreciated. I am also thankful to Dr. H. Tennekes and Mr. B. Khajeh-Nouri for their aid and supervision in Dr. Lumley's absence.

I wish to express my appreciation to Dr. R. E. Arndt for his help in designing the test tank exit and to Mr. Bruce Baker for his helpful discussions regarding the poly(ethylene oxide) solutions.

I am grateful to Shell Pipeline Division, Houston, for graciously providing the recording goniophotometer, and to Mr. R. Husted, Mr. T. Young, and Mr. E. Jordan for their time and indispensible technical assistance.

This research was supported by the U. S. Office of Naval Research, Fluid Dynamics Branch. The assistance of the Applied Research Laboratory in figure preparation is gratefully acknowledged.

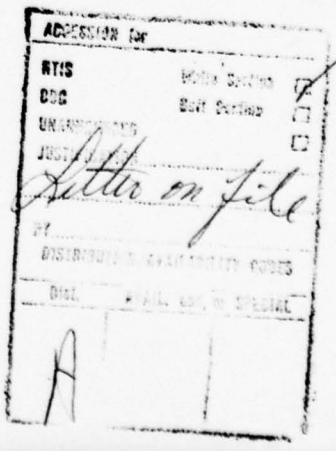

TABLE OF CONTENTS

LIST OF TABLES

LIST OF FIGURES

LIST OF SYMBOLS

c = concentration of the polymer additive

C = carbon molecule

f = friction factor

H = hydrogen molecule

I = intensity of scattered light

I_{pq} = variance tensor of position

O = oxygen molecule

r^2 = equilibrium mean-sqaure radius of the molecule

R_e = Reynolds number

S = strain rate

T = terminal relaxation time

u_k = local velocity

w_p = weight of polymer

w_w = weight of water

X,x = streamwise axis on position

x^i = fixed co-ordinate

$\overline{x^i}$ = transformed co-ordinate

Y,y = cross-stream axis or position

δ_{pq} = Kronecker delta

$[\eta]$ = intrinsic viscosity

θ = angle of scatter relative to main beam

μ = dynamic viscosity of solute

μ_s = dynamic viscosity of solvent

Ω = vorticity

CHAPTER I

INTRODUCTION

1.1 The Toms Phenomenon and Its Applications

Most natural and artificial fluid flows are characterized by turbulence that causes large energy losses due to the rapid mixing of the fluid's momentum (Tennekes and Lumley, 1972). These energy losses can increase the power requirement and the operating cost in a fluid system. For example, most of the power required to propel a ship through the ocean (at speeds well below the hull design speed) is dissipated by the excessive transport of momentum in the turbulent boundary layer that exists next to the ship's hull (Lumley, 1964a). This power loss limits the range and payload capabilities of the vessel. Similarly, the pressure drop along a pipe through which a turbulent flow occurs is much greater than it would be if the flow were maintained in a smooth, or laminar, condition. This pressure drop increases the pumping cost and limits the pressure and rate of flow in the system. Until 1948, little could be done to reduce these energy losses. However, at that time, B. A. Toms observed that when he measured the friction coefficient of a dilute solution of poly(methyl methacrylate) in monochlorobenzene (0.25% by weight) in turbulent flow through a pipe (see Figure 1), at a critical shear stress (same as

Reynolds number in Figure 1), friction was reduced to 50% compared to the pure solvent. This anomalous "phenomenon observed only in non-laminar flows" (Toms, 1948) has come to be known as the Toms Phenomenon. Since 1948, many other combinations of polymers and solvents at trace concentrations have been found to produce appreciable reductions in turbulent drag (see lists in Hoyt and Fabula, 1964). These polymer systems are generally inexpensive, nontoxic, and biodegradable, making them extremely attractive for military and commercial use. In particular, full-scale trial runs of a 140-foot coastal minesweeper, H.M.S. HIGHBURTON, showed a 12.7% reduction in ship resistence to the water when polymers were ejected from slots in the ship's hull near its bow (Canham, et al., 1971). In like manner, the New York City Fire Department has also taken advantage of the drag-reducing property of poly(ethylene oxide) in its Rapid Water Development Program. By injecting the polymer in the discharge side of a fire pump, the flow rate in a 2 1/2-inch hose has approached that in a 3 1/2-inch hose. In this way the polymer additive has enabled firefighters to use fire hoses that are lighter, more mobile, and smaller in diameter than usual (Clough, 1973). Different polymer additives have also been extensively used in oil pipeline technology as well (Ram, et al., 1967, Melton and Malone, 1964). The most important result, however, from these different polymer additives that demonstrate the Toms Phenomenon has been a source of much interesting

scientific research regarding the nature and structure of turbulence, itself.

1.2 Survey of Research

The study of the reduction of drag by polymer additives in turbulent fluid flow that spans almost three decades (Hoyt, 1972; Lumley, 1969; both have extensive reference lists) has greatly added to a deeper understanding of the fundamental principles of turbulent flows and polymer additives in nature and in their industrial applications. A joint effort of chemists and hydrodynamicists has been necessary to begin to explain the complex interaction between macromolecules and turbulent flows. These efforts have led to many explanations of this phenomenon.

B. A. Toms (1948) and J. G. Oldroyd (1948), both suggested that reduction in drag was caused by a "wall effect". They postulated that a shear-thinning wall layer of fluid near the wall caused low viscosity and allowed lower friction coefficients than in the pure solvent in similar flows. Later experiments have shown (Hoyt and Fabula, 1964; Pruitt and Crawford, 1963), however, that the viscosity of the solution remains essentially constant in solutions of concentration where reduction of friction occurs. Also, rheograms of solution of poly(ethylene oxide) and of guar showed by conventional measurement that these solutions were not shear-thinning but were (in this respect) Newtonian and yet still good drag-

reducing agents. Lumley (1964b) further demonstrated that turbulence cannot be appreciably affected by shear-induced changes in viscosity because inertia would dominate any viscous changes.

Elata and Poreh (1966) proposed that differences in normal stresses due to nonisotropic viscosity reduced the transfer of momentum in the turbulent boundary layer and could be a mechanism for reducing frictional drag. Differences in normal stresses have been measured (Metzner and Park, 1964; Gadd, 1965) in some polymer solutions, but Gadd (1966) has shown that solutions of polyacrylamide and of guar do not have measureable normal stress differences although the additives reduce friction in turbulent flows. Gadd concluded that there is no obvious correlation between normal stress differences and drag-reducing effects in polymer solutions.

One of the most promising of the explanations, however, has been to consider the macromolecules as being able to change shape elastically in the flow. Tulin (1966) postulated that the molecules would extend in the shear direction, thus, providing a stiffening effect to the flow and absorbing energy from the turbulent eddies; the energy would be radiated away in elastic shear waves that are damped by the solution's viscosity. Tulin suggested that the ability of the polymer molecules to dissipate energy could account for the decrease in turbulent intensity and, hence, the reduction in drag. Gadd (1965), likewise

conceived the macromolecules as relatively flexible chains having a spring-like nature that would make the fluid viscoelastic and thus affect the turbulence. Gadd, however, hypothesized that the mechanism of drag reduction does not dissipate turbulence but reduces turbulent production. Experiments, in fact, have shown (Bilgen, 1971) that there is a decrease in the population of small eddies in polymer solutions. Most importantly, however, Lumley (1969) and Peterlin (1970) have suggested that the most relevant mechanism is the actual change in relative size of the molecules in a fluctuating strain rate field of a turbulent flow. This extension of the molecules would provide a mechanism of the correct order of magnitude to account for the large effects of drag reduction (of order one) observed at dimensionaless concentrations many orders of magnitude less than unity. Lumley (1973) postulated that at a threshold shear stress, the rapidly changing rates of strain would cause the macromolecules to become extended, depending on concentration. The expanded molecules would then increase the effective viscosity of the solution and damp out the small eddies. This would lessen the Reynolds stress in the turbulent buffer layer and delay the reduction of the mean profile slope, causing an overall thickening of the sublayer. These changes would then account for the large anomalous reductions in turbulent frictional drag. As yet, however, there have been no

direct observations of the molecules as expanded to the extent predicted by Lumley's explanation of the drag-reduction process.

1.3. Purpose of the Investigation

Direct measurements of changes of molecular size of polymers in dilute solutions in simple shear flow have shown only a disappointingly small amount of stretching (Cottrell, et al., 1968, 1969, and 1970). However, Lumley (1972) has shown that no significant expansions of the polymer molecule should occur because in simple shear flow the vorticity and strain rate are equal and the molecules tend to rotate too fast past the principal axis of strain rate for the molecules to stretch. In general, however, turbulent flow contains all combinations of vorticity and strain rate so that a significant portion of the flow will be sufficiently rotation-free, to allow molecular stretching (Lumley, 1973, 1976). Based on this fact, the present investigation was to determine the elongations of the polymer molecules in a relatively rotation-free, pure straining flow at a strain rate above the threshold value to confirm the existence of molecular stretching as a possible drag-reducing mechanism. The investigation consisted of measuring the intensity and angle of light scattered by the polymer molecules in an aqueous solution as they passed through a thin beam of light normal to the centerline of a two-dimensional contraction used to produce the irrotational, pure straining flow. The intensity and angle

of diffracted light from the molecules in the strained and unstrained state were measured by a recording goniophotometer at five different positions along the centerline of the contraction. The rate of change of intensity with angle was then used to determine graphically the elongations of the polymer molecules. The poly(ethylene oxide) molecule was used exclusively as the polymer agent and was assumed to obey the Oldroyd equation (Oldroyd, 1950; Giesekus, 1962; Lumley, 1971; Gatski, 1976) to a first approximation for a theoretical comparison.

CHAPTER II

THE ADDITIVE, THE CONTRACTION, AND THE GONIOPHOTOMETER

2.1 The Polymer Additive

There are many polymer-solvent systems that demonstrate appreciable reduction in the effects of friction; however, only aqueous solutions of poly(ethylene oxide) were considered in this investigation because friction reductions of up to 75% have been measured (Fabula, 1965) in such solutions, making poly(ethylene oxide) one of the most effective drag-reducing agents known to date and a standard material for studies of reduced turbulence. This high-molecular weight, nonionic molecule has a simple linear structure (see Figure 2) that is extremely flexible, and is completely soluble in water and many other solvents. Poly(ethylene oxide) is also biodegradable, making it easily disposable. For this study, the polymer was obtained from the Union Carbide Corporation Chemical and Plastics Division, New York, under the trade name POLYOX WSR301, as a white granular powder. Only small amounts (about 25 pounds) were purchased at any one time to eliminate any degradation or contamination of the polymer sample.

The polymer was carefully mixed (see Chapter 3) with water to form a solution in which the isolated, unstrained poly(ethylene oxide) molecules were assumed to take a random-walk configuration; that is, the molecules form tangled,

"cotton-like" balls (see sketch (a) in Figure 3; an effective molecular diameter can be assigned from the light-scattering data). Under the straining action of turbulent flow, these "cotton-like" balls (filled mostly with solvent) tend to be stretched along the axis of principal strain rate because they are elastic and in general do not follow the fluid motion (see sketch (b) in Figure 3). As the molecules expand, two forces begin to act on them (Lumley, 1976): a drag force, produced by the relative flow of the medium over various parts of the molecule, and a restoring force, due to thermal agitation of the molecule. The latter acts like an internal spring force that tries to return the molecule to its original spherical shape. When the strain rate is large enough, the drag force overcomes the restoring force, and the molecule expands.

The restoring force is measured by the terminal relaxation time, T, which is the time constant for the molecule to return exponentially to spherical symmetry. If S is the strain rate, complete expansion in a steady flow takes place when 2ST first exceeds unity (Lumley, 1972). This strain rate is called the critical strain rate.

The drag force, due to the relative motion of the fluid past the molecules, represents a source of energy dissipation. This frictional energy loss appears as an increase in the effective viscosity of the solution (Debye, 1946). This change in viscosity of the solution alters the energy balance of the

turbulent flow such that there is a reduction in drag (Lumley, 1973).

2.2 The Contraction

The degree of strain experienced by the polymer molecules in a given flow field depends upon the relation between the molecular relaxation time and the characteristic strain rate of the flow field (Peterlin, 1966). It is essential that the time scale of the flow and the internal time scale of the molecules be of the same order of magnitude to allow interaction and leave the molecules aligned long enough with the axis of principal strain rate to produce sufficient stretching to account for the large drag-reducing effects.

Lumley (1972) has shown that significant molecular expansions should occur in a two-dimensional laminar flow if the molecules remain aligned with the principal axis of strain rate for a period of the order of the relaxation time. Such a flow, however, requires the fluid to be sufficiently free of rotation to allow the molecules to experience the strain long enough for extensions to occur. Figure 4 shows the criterion for molecular expansions in such a two-dimensional flow. The hyberbola, $\pm \sqrt{S^2 - \Omega^2} = \frac{1}{ST}$, is the threshold permitting an infinite expansion of the molecule in a steady, two-dimensional flow field. Unbounded expansion can only occur above the upper, or below the lower, branch of the hyberbola. Between its branches,

the vorticity is too great and the molecules rotate too quickly past the direction of maximum strain rate to allow unbounded stretching of the molecules.

To confirm the existence of sizable elongations of the molecules it is therefore necessary to have a flow field that can approach the criterion. The simplest flow field is one where the fluid is irrotational and the fluid particles only experience a pure straining motion. Such a flow field is produced in laminar flow along the centerline of a symmetric, two-dimensional contraction with the boundary co-ordinates derived by XY = constant. The strain rate is also constant, and the velocities are linearly proportional to the distance from the origin. Figure 5 shows the flow contraction used in this investigation. The contraction boundary is given by XY = 0.08, and the flow area is divided into three regions: a four-inch inflow region, a one-inch contraction region, and a three-inch outflow region. The inflow and outflow regions are necessary to insure uniform entrance and exit conditions. The entire flow apparatus is made of 3/16-inch thick, anodized aluminum clamped by plexiglass strips to two, 1/4-inch pyrex glass plates selected to withstand the pressure and allow clear passage of the diffracted light beam. The aluminum was anodized to eliminate any reaction with the polymer solution and also to provide a smooth surface at the walls. One pyrex plate was glued to the aluminum by a commercial epoxy to maintain the shape of

the contraction. The other pyrex glass plate was simply clamped by plexiglass strips and could be easily removed for cleaning the contraction between test runs. The glued pyrex glass plate, however, cracked due to out-of-the-plane stresses, so that it was necessary to glue a thin aluminum plate to the outside of the glass for support. A slot was machined in the plate in the area of the contraction to allow passage of the scattered optical beam. The plate was finally painted flat black to reduce any background scatter or secondary reflections (see Figure 5).

2.3 The Goniophotometer

The direct measurement of the size of the polymer molecule in the strained and unstrained state presents a challenging task. The task consists of measuring extremely small particles that have a relatively low refractive index, occur at trace concentrations, and are moving at relatively high flow velocities. In such a system, the suspended molecules cannot be clearly resolved. However, there is a simple light-scattering technique, based on established principles of light diffraction, that is well adapted for the characterization of such a difficult system (Sloan, 1953). The method has an important advantage for this study because the information that is obtained is relatively independent of both the refractive index and the concentration. It is also able to give size and size distributions over the important range of radii from 0.1 microns

to 100 microns in either a flowing or static system. The technique is an application of a theory proposed in 1908 by G. Mie that describes the angular refraction of light from nonconducting spheres in a medium. The method employs the principle that a given rate of change in intensity occurs with angle of scattered light from a given particle size. Figure 6 shows a schematic plot of intensity versus angle of scattered light for different relative particle sizes. If a particle is much smaller than 0.1 microns (marked "small" on the graph) the scattering of light is independent of angle of scatter, except for the polarization effect near 90°. At about 0.1 mircrons and larger, the scattering of light varies inversely with the particle size so that the rate at which the light intensity changes with angle can be used to determine its size. To illustrate this effect further, Figure 7 shows the effect of size and size distribution on the light-scattering curve. The figure schematically shows the scattering behavior to be expected of spheres of different sizes by using the Rayleight-Gans scattering equations, which are a useful approximation for the complete Mie theory treatment (Sloan, 1954; Arrington, 1954). For a particle of 1.0 micron radius, the drop in the logarithmic intensity curve becomes sharp at about 10°. For larger particles, this characteristic drop-off occurs at smaller and smaller angles; e.g., at 1° for 10 micron particles, 0.1° for 100-micron particles. The difference in the heights of the

intensity plateaus for the different particles serve to illustrate schematically the difference in absolute intensity of the scattered light produced by particles of different sizes. The most important fact is that the angular position of the characteristically steepening slope is determined by the size of the scattering particles (Sloan, 1954). The effect of a marked change in the concentration of the scattering particles is also illustrated by the broken lines showing the scattering obtained from lower concentrations of the same size particle.

While information about size can be obtained from the angular position of the knee in the log I versus log θ curve of Figure 7, the curve is even more informative if the constant intensity lines are given a pronounced negative slope, such as -2.0 (Sloan, 1954). This is done by plotting log $I\theta^2$ versus log θ, giving a maximum in the curve at the angular position characteristic of the size. Hoseman (1950) suggested this method of plotting the data for analyzing X-ray experiments. Since then, Arrington (1954) has shown that the $I\theta^2$ curve is proportional to the weight percent of the sample in a given size range and has concluded that Hoseman's method is also a useful approximation method of analyzing light-scattering data to obtain particle size and size distributions. Figure 8 illustrates this advantage by plotting the information of Figure 7 in this manner. The curves of all of the different size particles now have the same shape regardless of size. The

position of the respective main maxima on the log $I\theta^2$ plots can be used to introduce a scale of sphere sizes along the abscissa (note the inverse relation between size and angle). Further experimental evidence (Arrington, 1954) has also shown that this approach to interpreting the light-scattering data is satisfactory for not only monodisperse systems but also polydisperse samples. This makes the method suitable for the characterization of the polymer molecules in solutions used in this study.

The development of a special semi-automatic, high-resolution light-scattering instrument, produced by Leeds and Northrup, Philadelphia, called a goniophotometer, greatly aids the application of this method. The instrument is able to give an accurate, continuous recording of intensity of the scattered light from a given test sample at angles between 0.05° and 140° to the axis of the illuminating beam. A schematic diagram of the instrument and optical system is given in Figure 9. A narrow, well-defined optical beam, produced by a Spectra Physics 50 mw laser, is directed through a series of filters and slits where the beam impinges upon the test specimen, which causes the light beam to be diffracted and scatters light throughout the device. The intensity of scattered light is then measured by a photo-multiplier tube attached to a rotating arm that continuously scans the pattern of scattered light at various angles and at various scanning rates. Small angle light-scattering

measurements are made using slow scaning speeds and narrow slits for high resolution, while intermediate and large-angle scattering measurements are made with progressively higher scanning rates and wider slit widths. The intensities are recorded and corrected for the solvent, then plotted on the log $I\theta^2$ plots. From the plots, the data can be readily analyzed for particle size and size distribution.

CHAPTER III

EXPERIMENTAL SET-UP, PROCEDURE, AND RESULTS

3.1 Set-Up

The experimental set-up for this investigation was a system in which the polymer solution could be thoroughly mixed and allowed to flow at a constant flow rate through the two-dimensional contraction where light scattering was continuously measured by a recording goniophotometer surrounding the contraction. The system consisted of a mixing tank, a pressurized test tank, a smooth connecting pipe, a two-dimensional contraction, and a goniophotometer, which includes a high impedance recorder and a laser light source (see Figure 10).

The 120-gallon, wooden mixing tank (see Figure 11) was lined with a water-proof plastic liner, which was replaceable in case of a leak or excessive build-up of undissolved waste polymer. All solutions used in the test runs were mixed in this tank by a mechanical stirring unit located on top of the mixing tank. The mixer had a paddle made of two thin, metal blades (18.0-inches by 2.5 inches) connected in parallel. The paddles were designed to stir the solution at a rate (22 r.p.m.) that would not break the large polymer chains. The mixing tank was connected to the 120-gallon pressurized test tank directly below

by a short length of 2.0-inch (I.D.) galvanized pipe and a 2.0-inch gate valve.

The aluminum pressurized test tank (2.0 feet x 2.0 feet x 4.5 feet) had a reinforced plexiglass front that allowed observation of the solution level at all times during the test runs (see Figure 12). The inside of the tank was painted to eliminate corrosion of the tank by the polymer solution. The (4.5 feet) height of the solution in the test tank and (2.5 psi) pressurization by a regulated nitrogen gas system combined to give a total head large enough to produce the desired flow rate through the two-dimensional contraction. The solution exited from the tank under pressure through a smooth entrance piece (see Figure 13) machined to follow the streamlines of a vena contracta (Lamb, 1945). The smooth entrance piece was connected to the lower face of the reinforced plexiglass front. A 2.0-inch (I.D.) ball value, attached to the smooth entrance piece, opened and closed the system (see Figure 14). Both the entrance piece and the ball value allowed the solution to remain laminar as it flowed from the test tank into the two-dimensional contraction.

A 5-foot long, 2.0 inch diameter (I.D.) plexiglass tube connected the ball valve to the two-dimensional test contraction. The Reynolds number in the tube was about 680. This value was based on the diameter of the tube and a solution viscosity obtained from the definition of the intrinsic viscosity of a polymer solution:

$$\mu = \mu_s(1 + c[\eta])$$

where c is the concentration, μ_s is the viscosity of the solvent, μ is the viscosity of the solution and $[\eta]$ is the intrinsic viscosity (taken as 20.0 dl/g for WSR 301, see Virk, et al. 1967). At this Reynolds number, the short length of the tube permitted the flow to enter the test contraction with a fairly flat mean velocity profile.

A round-to-rectangular smooth transition piece (2.0-inch to 2.0 x 0.2 inches) connected the plexiglass tube to the test contraction (see Figure 15). The contracting of the flow by the transition piece occurred in a plane normal to the plane of the two-dimensional test contraction.

The two-dimensional test contraction was bolted to the smooth connecting tube by the transition piece and was positioned inside the goniophotometer (see Figure 16) at 90° to the light source (a He-Ne laser). The test contraction could be adjusted slightly up or down to allow the light beam to strike the centerline of the contraction (see Figure 17). However, to move the beam along the centerline of the contraction, the whole goniophotometer had to be repositioned for each location. The downstream end of the contraction was flanged to a short length of plexiglass pipe that extended through a hole in the wall of the goniophotometer and emptied into an open drain.

The goniophotometer that surrounded the two-dimensional contraction was extensively modified for the flow-through set-up. The stationary test cell was removed and replaced by the

pyrex glass contraction. An adjustable mounting table was constructed to allow proper positioning of the test contraction over the axis of rotation of the scanning arm and perpendicular to the light beam (see Figure 18). Holes were cut in the front and back walls of the apparatus to permit the use of the flow-through system. These holes were made light-tight by covering the pipes with black paper and using black rubber flanges that fit tightly to both the pipes and the wall of the goniophotometer. The light source of the goniophotometer was changed from a mercury-arc lamp to a Spectra-Physics model 125A (50 mw) He-Ne gas laser (see Figure 19) because the laser produced a sharper, more intense beam of light than the lamp. Finally, additional modifications were made to the recording system of the goniophotometer by replacing the original Leeds and Northrup Speedomax Type G recorder with a high impedance Brüel and Kjaer level recorder Type 2305 (see Figure 20). The performance capabilities of the goniophotometer were also limited by the flow-through system. With the contraction and connecting tubes in place, the scanning range was reduced to 0° to 90°. However, scattering data was needed only from light scattered between 2° to 30°. The goniophotometer was also equipped with a series of neutral density filters (see Figure 9 and 21) which could be used to control the intensity of the incident light reaching the photomultipler tube by steps of two over a range of as much as 73,000 but these filters were not

needed over the scanning range of 2° to 30° since the intensity of scattered light was low enough so that the necessary signal attenuation could be done by the recording unit itself. These filters were only used to measure the main beam intensity at 0° (see Section 3.3).

3.2 Procedure

The procedure for this experiment was in two phases: the solution preparation and the recording of the light-scattering data. The same procedure was followed for five different positions (.4, .6, .66, .75, .85) measured in inches from the origin (see Figure 5) along the centerline of the contraction. Two complete test runs were done at each position to confirm the reliability of the light-scattering data. A complete test run included a water-control run, a still polymer solution run, and a moving polymer solution run. The moving runs were performed at an exit bulk velocity of 19.2 feet per second, giving a 2ST value close to unity for the poly(ethylene oxide) molecule and this contraction. Two complete test runs required 100 gallons of polymer sclution.

The preparation of the polymer solution consisted of mixing two, 120-gallon batches of tap water and polymer at a concentration of 1600 ppmw. These batches were mixed one at a time in the mixing tank with the stirring unit. The concentration for the two mixtures were determined as follows:

$$c = \frac{w_p}{w_w} 10^{-6}$$

where, c is the concentration per million, w_p is the weight of the polymer, and w_w is the weight of the water. The proper amount of poly(ethylene oxide) powder was weighed out and allowed to fall through a fine screen, a procedure which produced a small cloud of polymer particles inside the mixing tank. The cloud was then dispersed and mixed into solution by a fine but forceful spray of water before the polymer particles reached the surface of the water in the mixing tank. In this way the polymer particles were completely dissolved, resulting in a fairly consistent mixture each time. The solution was then lightly stirred for two hours by the stirring unit. After stirring was completed, the first batch was allowed to drain into the test tank so that a second batch at the same concentration could be prepared in the same manner. After both batches had been stirred, they were left to stand overnight so that the polymer was thoroughly hydrolized. The resulting solution had an opacity close to that of water.

When the polymer solution was ready, measurements of light scattering were made with the goniophotometer. The first measurements were taken for a still polymer solution. The ball valve was slowly opened, which allowed the contraction to fill. A butter-fly valve in the exit pipe was closed to keep the solution from escaping while a bleeder valve on the contraction was opened to allow the air to be pushed out of the system as the contraction and connecting tubes filled with the polymer

solution. Once the system was full (ball valve closed) and all motion within the system had damped out, the goniophotometer was sealed and light scattering measurements were taken by scanning the pattern of light scattered by the still polymer solution from 0° to 30°. Two scanning rates were used to make this measurement: a rate of 4°/minute from 0° to 15° and a rate of 20°/minute from 15° to 30°.

The signal from the photomultiplier tube was recorded at a constant rate (1.0 mm/sec) on a strip chart in real time. (For more details see Section 3.3 and Figure 22.) The recorder attenuated the signal at the same set angles for all runs to allow easy comparison of signal changes. The angle as well as the intensity were recorded on the strip chart. The solution was scanned twice to insure reliable results, and a third run was made if there were large differences in the first two recorded patterns of scattered light.

After the still polymer runs were completed data were gathered for the moving polymer solution. For this run the test tank was filled to the top and pressurized with 2.5 psi of nitrogen gas. After pressurization was completed the ball valve and the butter-fly valve of the exit tube were opened to allow the polymer solution to flow through the contraction with an exit velocity of 19.2 feet per second (average bulk velocity). Air bubbles were released from the bleeder valve on the contraction. The goniophotometer was sealed and measurements of

light scattering were taken for two runs in the same manner as for the still polymer solution. The second run was made by refilling the test tank and repressurizing it to maintain the same bulk velocity for both runs.

Once runs were completed for the still and moving polymer solutions, the system was drained and washed with clear tap water. The contraction was then disconnected from the system at the flanges to the connecting tube and the exit tube. The disconnected test contraction was dismantled and was thoroughly cleaned. After cleaning the contraction was plugged at both ends and filled with clear tap water. The filled contraction was then sealed and reconnected to the system and measurements of light scattering were taken with only still water in the contraction. This water control run was made in the same manner as those with the still polymer. When all the runs were completed for one position, the goniophotometer was repositioned at the next location and the entire procedure was repeated.

3.3 Results

Figure 22 shows a typical pattern of light scattering for a still polymer solution. The peak at 0° is the intensity of the main beam maximally attenuated by the neutral density light filters of the goniophotometer. These filters reduce the intensity by a faction of about 73,000 so that the photomultiplier tube can record the full intensity of the main

beam, a measurement necessary to determine the percent transmission of the sample (this concept will be discussed later). The rest of the pattern of light scattering was recorded between 2° and 30°; this pattern was recorded without any attenuating filters in the path of the main beam so that only the recorder's attenuation was used to keep the signal in the operational range of the recorder. Each step of attenuation in Figure 22 is a reduction in the signal by 10 db. The range of scan was chosen to give data only in the size range of the poly(ethylene oxide) molecules (i.e., 0.2 microns to 5.0 microns). Two scanning rates were used in making the measurements: 4°/minute between 0° and 15° and 20°/minute between 15° and 30°. Also in Figure 22, the scattering pattern for the water control solution (pure solvent) was traced on the same chart to demonstrate the effect the polymer molecules have on the pattern of light scattering. The higher intensity of light for any given angle for the polymer solution compared to the pure solvent is due to the presence of the poly(ethylene oxide) molecules. The relative difference between the two signals is affected by the concentration of the polymer solution. Because the scattering cross section for a given polymer molecule is small, a rather high concentration of 1600 ppmw was required to give a reliable difference in signals between the two solutions. Such a high concentration would

affect the behavior of the polymer in a drag-reducing turbulent flow, but here there should be relatively little effect.

Once the patterns of light scattering for the water control, still polymer solution, and moving polymer solution were obtained for a given position along the centerline of the two-dimensional contraction, the elongation of the polymer molecules was determined by plotting the intensity of light with angle of scatter on Log $I\theta^2$ charts (see Section 2.3) and then comparing the size distribution for the still polymer solution to that of the moving polymers solution. To convert intensity values from the recordings to the Log $I\theta^2$ plots involved correcting for light scattered from the solvent. The correction is made by first calculating the transmission of the sample, which is the ratio of the intensity of the main beam transmitted by the polymer solution to the intensity of the main beam transmitted by the water control (pure solvent). This transmission is the basis for determining the extent to which correction for the solvent must be applied to the polymer solution so that only the scatter due to the polymer molecules is obtained. This is done by multiplying the water-control intensity at a particular angle by the transmission and substracting this value from the intensity for the polymer solution at the same angle. The corrected intensity, due now only to the polymer molecules, can be directly plotted with

angle on the Log $I\theta^2$ charts so that particular sizes can be readily determined.

Figures 23 through 27 show the data reduced in this way for all five positions (.4, .6, .66, .75, .85) measured in inches from the origin (see Figure 5) along the centerline of the two-dimensional contraction. Both still and moving polymer solutions are plotted on the same graph to determine the shift in distributions of size between the two solutions (i.e. unstrained state and strained state) due to the irrotational straining action of the contraction. The Log $I\theta^2$ plots all show characteristically the same shape. There is definitely a distribution of size (polydispersion) for any given sample, but all the samples are within the same distribution of relative size for a given mixture. To determine changes in size, the largest possible size is used; this size is determined by the position of the point where the intensity distributions tend to go parallel to a constant intensity line (i.e., where the slope of the data curve approaches -2.0) with the magnitude of the radius of the molecules being read from the scale for determining spherical shapes (i.e., first scale on abscissa). All five plots show the largest still (unstrained) polymer molecules to be approximately 0.8 microns in diameter, while the size of the largest moving (strained) polymer molecules varies according to the position along the centerline of the two-dimensional contraction. Table 1 lists the molecular sizes

(strained and unstrained) and the corresponding elongations determined from the Log $I\theta^2$ plots for the five positions.

Table 1

Molecular Extension Data

Centerline Position (in)	Molecular Size (microns)		Molecular Elongation
	Unstrained	Strained	
0.4	0.85	1.60	1.88
0.6	0.85	2.00	2.35
0.66	0.90	2.60	2.89
0.75	0.85	3.20	3.76
0.85	0.95	1.65	1.74

Figure 28 shows a plot of elongation versus distance along the centerline. In order to make a comparison between the measured elongations and predicted elongations for the same estimated 2ST value, the solid line in Figure 28 represents the calculated values of the molecular size from the Oldroyd equation, which is known to be a first approximation of the constitutive relation for a polymer solution and is generally used to determine molecular size (Lumley, 1971; Gatski, 1976). These values were calculated by a finite element method using a

relaxation time that gave the best fit to the data (see Appendix A for details). This relaxation time is of the order of the largest times measured for this polymer by Berman et al. (1973), making the experimental values in good agreement with the Oldroyd equation. The measured values are within the range of deviation expected for light scattering measurements. However, some of the deviations are probably due to geometric imperfections in the construction of the nozzle. These inaccuracies effect the flow field which in turn effects the elongation of the polymer molecules.

CHAPTER IV

SUMMARY AND CONCLUSION

As previously mentioned, extreme stretching of polymer molecules has been postulated as the basic drag-reducing mechanism in turbulent flows of dilute polymer solutions. The stretching is predicted to occur in significant portions of the turbulent flow where the strain rate field is sufficiently rotation-free and above the threshold for the particular polymer additive. The relative flow over the extended molecules would increase the effective viscosity, which in turn would alter the turbulent boundary layer and cause a large reduction in drag. To provide support for these predictions, the explicit purpose of this investigation was to determine experimentally the streamwise extensions of poly(ethylene oxide) molecules in such an isolated strain rate field. This was done by obtaining distributions of molecular size from measuring the pattern of light scattered by illuminated polymer molecules flowing along the centerline of a two-dimensional, irrotational contraction. The actual experiment consisted of using a modified goniophotometer to record the light scattering pattern and, then, graphically determining the distribution of molecular size for the poly(ethylene oxide) test solutions using basic principles of optical physics. Elongations of up to

approximately four times the original molecular size were measured in this way.

These elongations were approximately those predicted by the Oldroyd equation. The extensions were not large, due to the low 2ST value, but the good agreement indicates that the Oldroyd model gives an accurate description of the stretching behavior of the molecules, suggesting that large extensions can be expected at higher 2ST values. These measurements verify for the first time the actual existence of molecular stretching large enough to account for the anomalous reductions in turbulent drag experienced by flowing dilute polymer solutions.

APPENDIX A

FINITE ELEMENT FORM OF THE OLDROYD EQUATION FOR DETERMINING MOLECULAR EXTENSIONS

A dumbell model consisting of two masses held together by an elastic restoring force has been generally used to model the polymer molecules in dilute solution. On the basis of this simple model and the assumption that the inertia of the molecule can be neglected, a theoretical estimate has been formulated (Lumley, 1971) for the deformation of polymer molecules in turbulence in a form relating to Oldroyd's constitutive equation. Lumley (1972) has shown that such an estimate is obtained by considering in an arbitrary flow the equation governing the moment-of-inertia tensor of the probability density of the molecule's end-to-end location. The appropriate equation relative to a fixed reference frame is:

$$\frac{\partial I_{pq}}{\partial t} + I_{pq,k}u_k - I_{p,}u_{q,j} - I_{qj}u_{p,j} + \frac{I_{pq}}{T} = \frac{\delta_{pq}r^2}{3T} \qquad (1)$$

where, $u_{p,j}$ is the local velocity gradient, T is the terminal relaxation time, and r^2 is the equilibrium mean-square radius of the molecule. The moment-of-inertia tensor of position, I_{pq}, represents the mean square location of mass relative to the center of mass for the dumbell model, so that the square root of the diagonal elements gives a measure of the molecular

extension. A finite element method of solution of Equation (1) for the two-dimensional flow field used in this study (see Section 2.2) was applied to give the predicted values shown in Figure 28.

From Equation 1, an equation describing the deformation of the polymer molecule undergoing steady axi-symmetric strain along the centerline of the two-dimensional contraction is obtained by considering the time independent, streamwise component (I_{11}) distribution along the principle axis of strain-rate:

$$u_1 \frac{dI_{11}}{dx_1} - (2S - \frac{1}{T}) I_{11} = \frac{r^2}{3T} \qquad (2)$$

where S is the local strain rate in the streamwise direction along the centerline. Equation 2 can now be readily applied to a finite element method of solution since Gatski (1976) has provided a theoretical estimate for the velocity field through the same two-dimensional contraction used in this experimental study. Figure 7 in Gatski gives the plot of the streamwise non-dimensional strain rate S^{11} which was used to determine u_1 and S in Equation 2.

To apply the method of finite elements in order to obtain a distribution of molecular extensions along the centerline of the contraction, the solution to Equation 2 must first be determined. This can easily be done by using a simple transformation by letting:

$$\frac{dx_1}{u_1} = d\bar{x}_1 \qquad (3)$$

Equation 2 now transforms into a readily soluable form:

$$\frac{dI_{11}}{d\bar{x}_1} - (2S - \frac{1}{T})\, I_{11} = \frac{r^2}{3T} \tag{4}$$

The solution to Equation (4) is therefore in non-dimensional form (for constant S):

$$\frac{3I_{11}}{r^2} = \frac{1}{1 - 2ST} + \frac{3I^{\circ}_{11}}{r^2}\, e^{(2S - \frac{1}{T})\bar{x}_1} \tag{5}$$

where $\frac{3I^{\circ}_{11}}{r^2}$ is any initial shape distortion from equilibrium. The method of finite elements was then applied by dividing the contraction into eight separate element s(Δx) in each of which the strain rate was considered constant. A velocity distribution across each element was determined as:

$$u_1 = u^{\circ}_1 + Sx_1 \tag{6}$$

where u°_1 is the velocity entering the element. Substituting Equation 6 into Equation 3 and integrating across an element the non-dimensicnal deformation of a polymer molecule across an element is given from Equation 5 as:

$$(\frac{3I^{f}_{11}}{r^2})^{\frac{1}{2}} = (\frac{1}{1 - 2ST} + \frac{3I^{\circ}_{11}}{r^2}\, (1 + \frac{S\Delta x}{u^{\circ}})^{2 - \frac{1}{ST}})^{\frac{1}{2}} \tag{7}$$

Element by element calculation with Equation 7 using the data supplied by Figure 7 in Gatski generated the curve found in Figure 28 by matching each element at their corresponding end points.

REFERENCES

Arrington, Jr., C. H., "Angular-Dependence Light Scattering. III Interpretation of Scattering From Monodisperse Systems," Contribution No. 353 from the Chemical Department Experimental Station, E. I. duPont de Nemours and Company, Wilmington, Delaware, 1954.

Bilgen, E., "Stability of Three-Dimensional Boundary Layer of Dilute Polymer Solutions," Journal of Basic Engineering, Trans. ASME, Series D, Vol. 93, No. 2, Mar. 1971, p. 85.

Canham, H. J. S., Catchpole, J. P., and Long, R. F., "Boundary Layer Additives to Reduce Ship Resistance," The Naval Architect, J. Rina, No. 2, July 1971, p. 187.

Clough, T. C., "Research on Friction Reducing Agents," Fire Technology, Vol. 9, No. 1, Feb. 1973, pp. 32-45.

Cottrell, F. R., "An Experimental Study of the Conformation of Polyisobutylene in a Hydrodynamic Shear Field," ScD thesis, Massachusetts Institute of Technology, 1968.

Cottrell, F. R., Merrill, E. W., and Smith, K. A., "Conformation of Polyisobutylene in Dilute Solution Subjected to Hydrodynamic Shear Field," Journal of Polymer Science, Series A-2, Vol. 7, 1969, p. 1417.

Cottrell, F. R., Merrill, E. W., and Smith, K. A., "Intrinsic Viscosity and Axial Extension Ratio of Random-Coiling Macromolecules in a Hydrodynamic Shear Field," Journal of Polymer Science, Series A-2, Vol. 8, 1970, p. 287.

Debye, P., "The Intrinsic Viscosity of Polymer Solutions," Journal of Chemical Physics, Vol. 14, No. 10, 1946, pp. 636-639.

Elata, C., and Poreh, M., Momentum Transfer in Turbulent Shear Flow of an Elastico-Viscous Fluid," Rheologica Acta, Vol. 5, 1966, p. 148.

Fabula, A. G., "The Toms Phenomenon in the Turbulent Flow of Very Dilute Polymer Solutions," Proceedings Fourth International Congress on Rheology, 1963, Part 3, Lee, E. H., ed., Interscience Publishers, New York, 1965, p. 455.

Gadd, G., "Difference in Normal Stress in Aqueous Solutions of Turbulent Drag Reducing Additives," Nature, Vol. 212, 1966, p. 1348.

Gadd, G. E., "Turbulence Damping and Drag Reduction Produced by Certain Additives in Water," Nature, Vol. 206, 1965, p. 463.

Gatski, T., "The Numerical Solution of the Steady Flow of Newtonian and Non-Newtonian Fluids through a Contraction," Ph.D. Thesis, Aerospace Engineering, The Pennsylvania State University, 1976.

Giesekus, H., "Elasto-viskose Flüssigkeiten, Für Die In Stationaren Schichtströmungen Sämtliche Normalspannungs-Komponenten Verschieden Gross Sind," Rheologica Acta, Vol. 12, No. 1, 1962, pp. 50-62.

Hoseman, R., "Röntgeninterferenzen an Kolloiden Systemen," Kolloid-Zeitschnift, Vol. 117, 1950, pp. 13-41.

Hoyt, J. W., and Fabula, A. G., "The Effect of Additives on Fluid Friction," Proceedings Fifth Symposium on Naval Hydrodynamics, Bergen, Norway, Office of Naval Research, ACR-112, 1964, pp. 947-974.

Hoyt, J. W., "The Effect of Additives on Fluid Friction," Journal of Basic Engineering, June 1972, pp. 258-285.

Lamb, H., Hydrodynamics, Dover Publications, New York, 6th ed., 1945, p. 99.

Lumley, J. L., "Applicability of the Oldroyd Constitutive Equation to Flow of Dilute Polymer Solutions," The Physics of Fluids, Vol. 14, No. 11, 1971, pp. 2282-2284.

Lumley, J. L., "Drag Reduction by Additives," Annual Review of Fluid Mechanics, Vol. 1, 1969, pp. 367-384.

Lumley, J. L., "Drag Reduction in Turbulent Flow by Polymer Additives," Journal of Polymer Science: Macromolecular Reviews, Vol. 7, 1973, pp. 263-290.

Lumley, J. L., "On the Solution of Equations Describing Small Scale Deformation," Symposia Mathematica, Vol. 9, Academic Press, New York, 1972, pp. 315-334.

Lumley, J. L., "The Reduction of Skin Friction Drag," Proceedings Fifth Symposium on Naval Hydrodynamics, Bergen, Norway, Office of Naval Research, ACR-112, 1964a, pp. 915-928.

Lumley, J. L. "Turbulence in Non-Newtonian Fluids," Physics of Fluids, Vol. 7, 1964b, p. 335.

Lumley, J. L., "Two-Phase and Non-Newtonian Flows," Topics in Applied Physics, Vol. 12, Turbulence, Chapter 7, P. Bradshaw, ed., Springer-Verlag, Heidelberg, 1976.

Melton, L. L. and Malone, W. T., "Fluid Mechanics Research and Engineering Application in Non-Newtonian Fluid Systems," Society of Petroleum Engineering Journal, 1964, p. 56.

Metzner, A. B., and Park, M. G., "Turbulent Flow Characteristics of Viscoelastic Fluids," Journal of Fluid Mechanics, Vol. 20, 1964, p. 291.

Mie, G., "Beiträge zur Optik trüber Medien, speziellkolloidaler Metallösungen," Annalen Der Physik, Vol. 25, No. 3, 1908, pp. 377-445.

Oldroyd, J. G., "A Suggested Method of Detecting Wall-Effects in Turbulent Flow through Tubes," Proceedings First International Rheological Congress, Holland, Part II, 1948, pp. 130-134.

Oldroyd, J. G., "On the Formulation of Rheological Equations of State," Proceedings of the Royal Society, London, Vol. A200, 1950, pp. 523-541.

Peterlin, A., "Hydrodynamics of Linear Macromolecules," Journal of Pure and Applied Chemistry, Vol. 12, 1966, pp. 563-586.

Peterlin, A., "Molecular Model of Drag Reduction by Polymer Solutes," Nature, Vol. 227, 1970, p. 598.

Pruitt, G. T., and Crawford, H. R., "Drag Reduction. Rheology, and Capillary End Effects of Some Dilute Polymer Solutions," Westco Research Final Report on Contract 60530-8250 to Naval Ordnance Test Station, 1963.

Ram, A., Finkelstein, E., and Elata, C., "Reduction of Friction in Oil Pipe-lines by Polymer Additives," I & EC Process Design and Development, Vol. 6, 1967, p. 309.

Savins, J. G., "Some Comments on Pumping Requirements for Non-Newtonian Fluids," Journal of the Institute of Petroleum, Vol. 47, 1962, p. 329.

Sloan, C. K., "Angular-Dependence Light Scattering. I. Characterization of Disperse Systems Containing Particles 0.1 to 100 Microns in Radius," Contribution No. 351 from the Chemical Department, Experimental Station, E. I. duPont de Nemours and Company, Wilmington, Delaware, 1953.

Sloan, C. K., "Angular-Dependence Light Scattering II. Characterization of Typical Disperse Systems" Contribution No. 352 from the Chemical Department Experimental Station, E. I. duPont de Nemours and Company, Wilmington, Delaware, 1950.

Tennekes, H. and Lumley, J. L., A First Course in Turbulence, M.I.T. Press, Cambridge, 1972.

Toms, B. A., "Some Observations on the Flows of Linear Polymer Solutions through Straight Tubes at Large Reynolds Numbers," Proceedings First International Congress of Rheology, Holland, Part II, 1948, pp. 135-141.

Tulin, M. P., "Hydrodynamics Aspects of Macromolecular Solutions," Proceedings Sixth Symposium on Naval Hydrodynamics, Washington, ONR ACR-136, 1966, p. 3.

Virk, P. S., Merrill, P. S., Mickley, H. S., Smith, K. A., and Mollo-Christensen, E. L., "The Toms Phenomenon: Turbulent Pipe Flow of Dilute Polymer Solutions," Journal of Fluid Mechanics, Vol. 30, part 2, 1967, pp. 305-328.

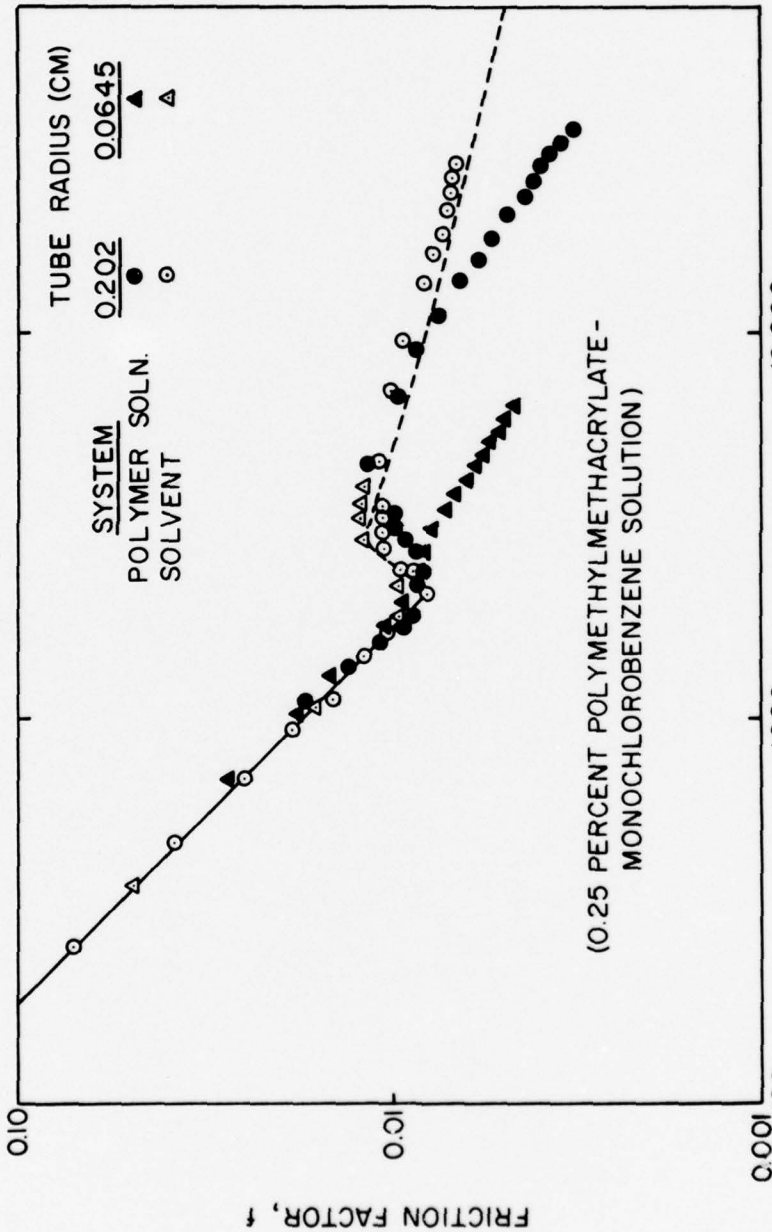

Figure 1. Experimental Data of B. A. Toms (Replotted from Savins, 1966).

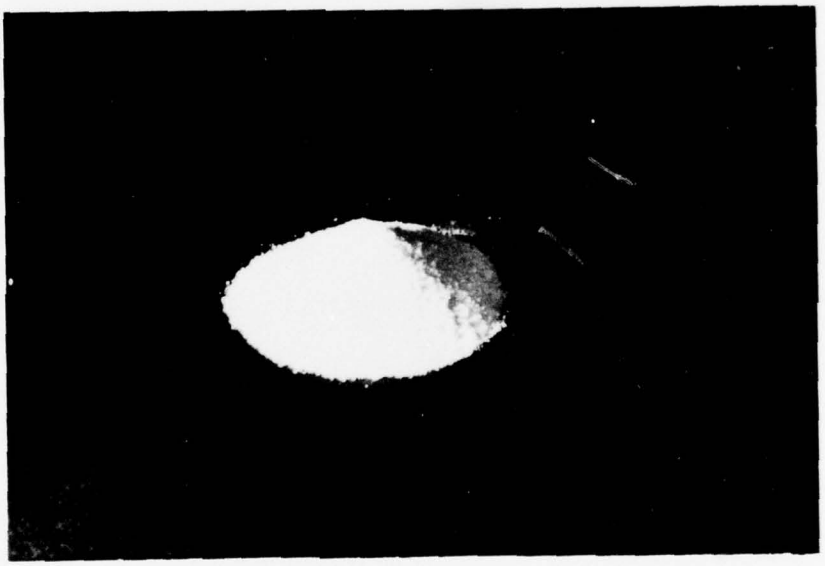

$$-O-CH_2-CH_2-O-\left[CH_2-CH_2-O\right]_N-CH_2-CH_2$$

Figure 2. Powder Sample and Chemical Formula of Poly(ethylene oxide) WSR 301 (Molecular Weight (Approx.): 4,000,000).

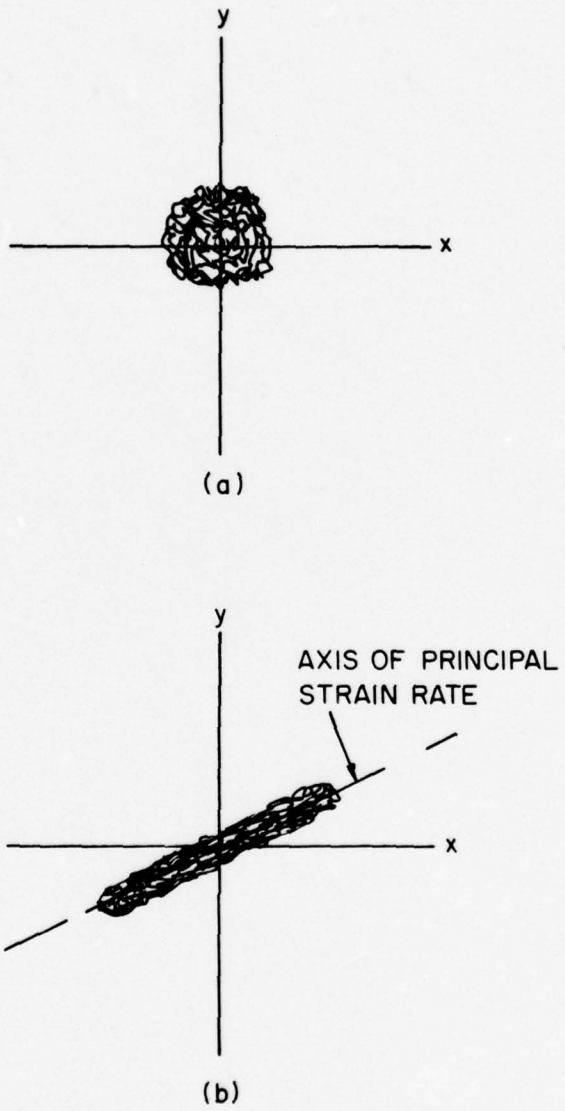

Figure 3. Sketches of the Unstrained (a) and Strained (b) State of the Polymer Molecules in Solution.

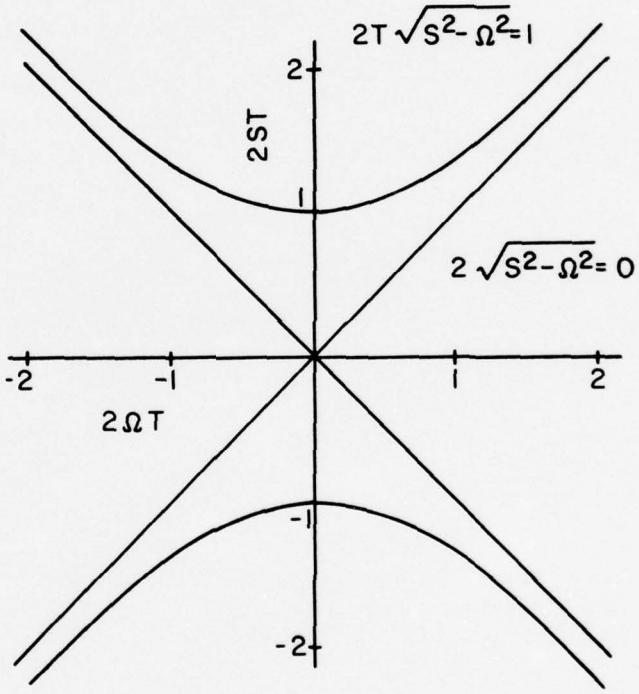

Figure 4. The Criterion for Molecular Expansion in a Two-Dimensional Flow (Lumley, 1972).

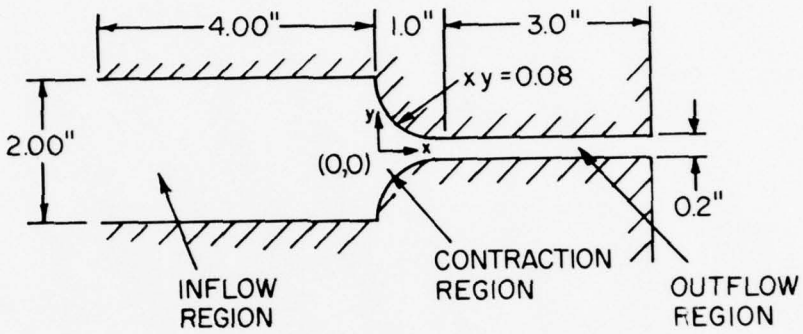

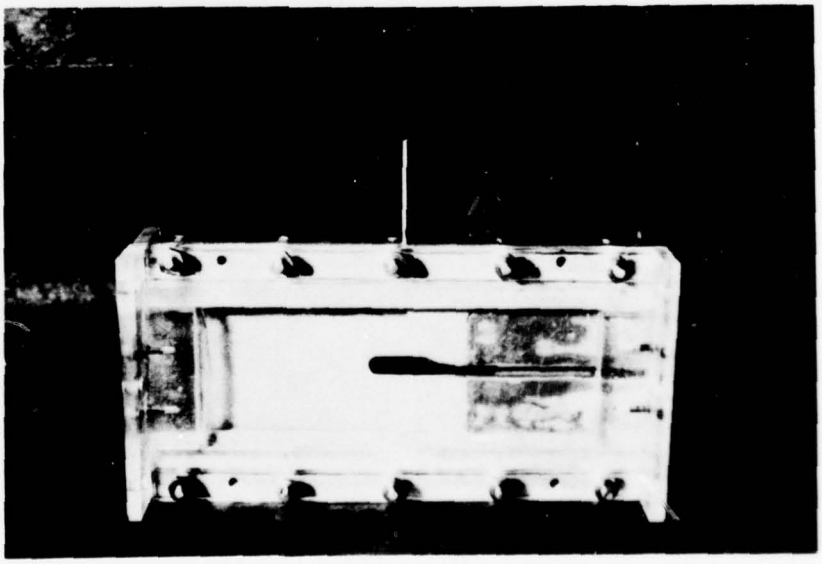

Figure 5. Diagram and Photograph of the Two-Dimensional Contraction.

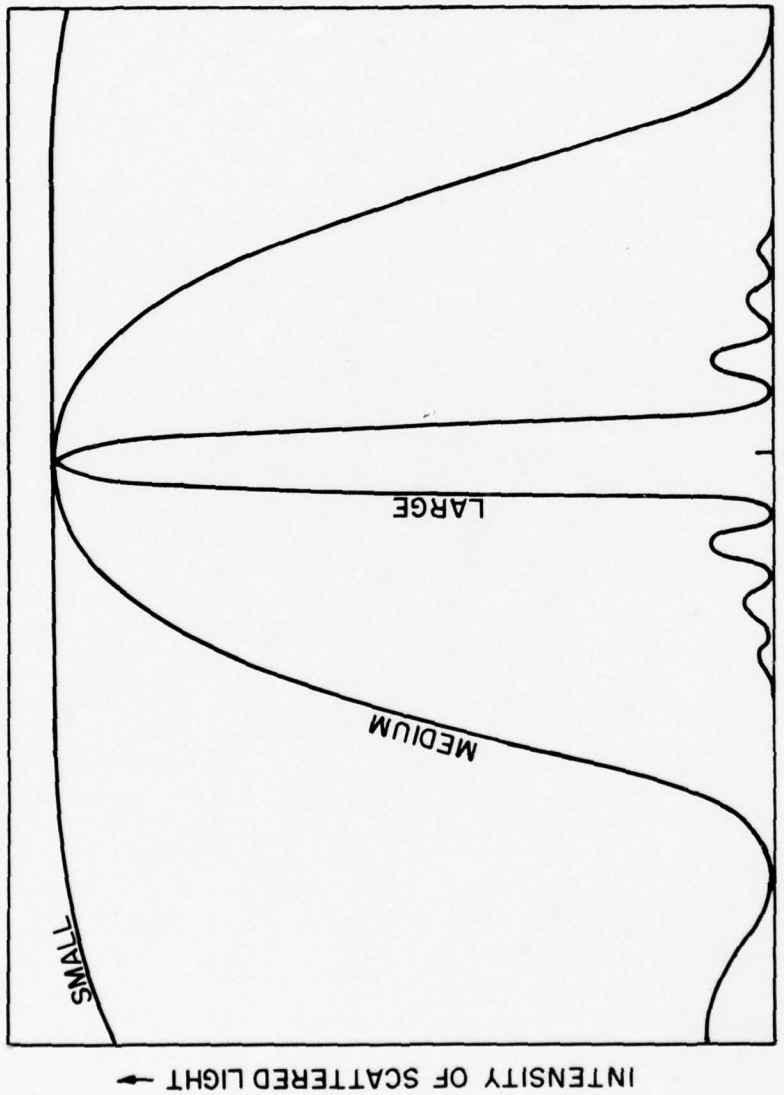

Figure 6. Schematic Plot of Intensity of Scattered Light Versus Angle of Scatter for Different Relative Particle Sizes.

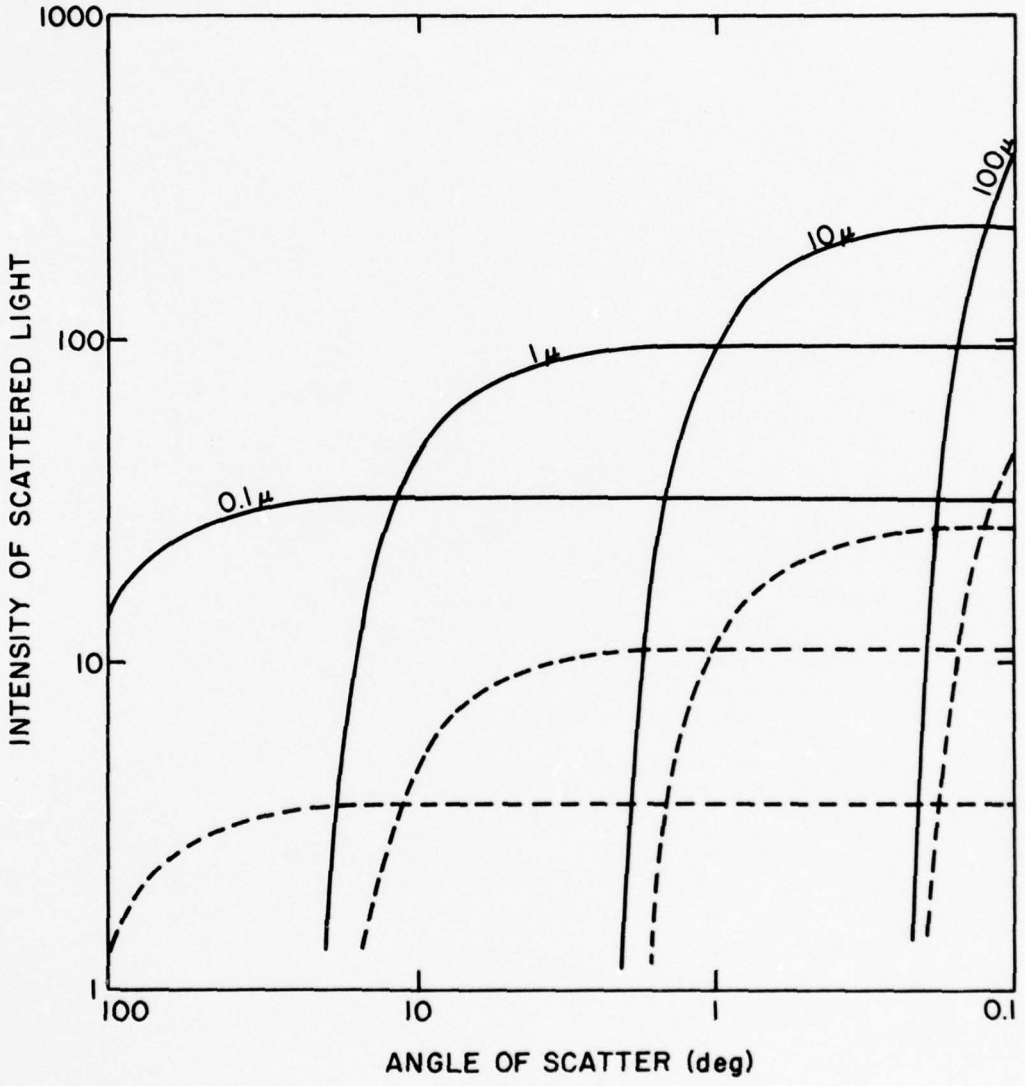

Figure 7. Schematic Plot of the Scattering Behavior of Spheres of Different Sizes and Concentrations Using the Rayleigh-Gans Scattering Equations (Sloan, 1954a).

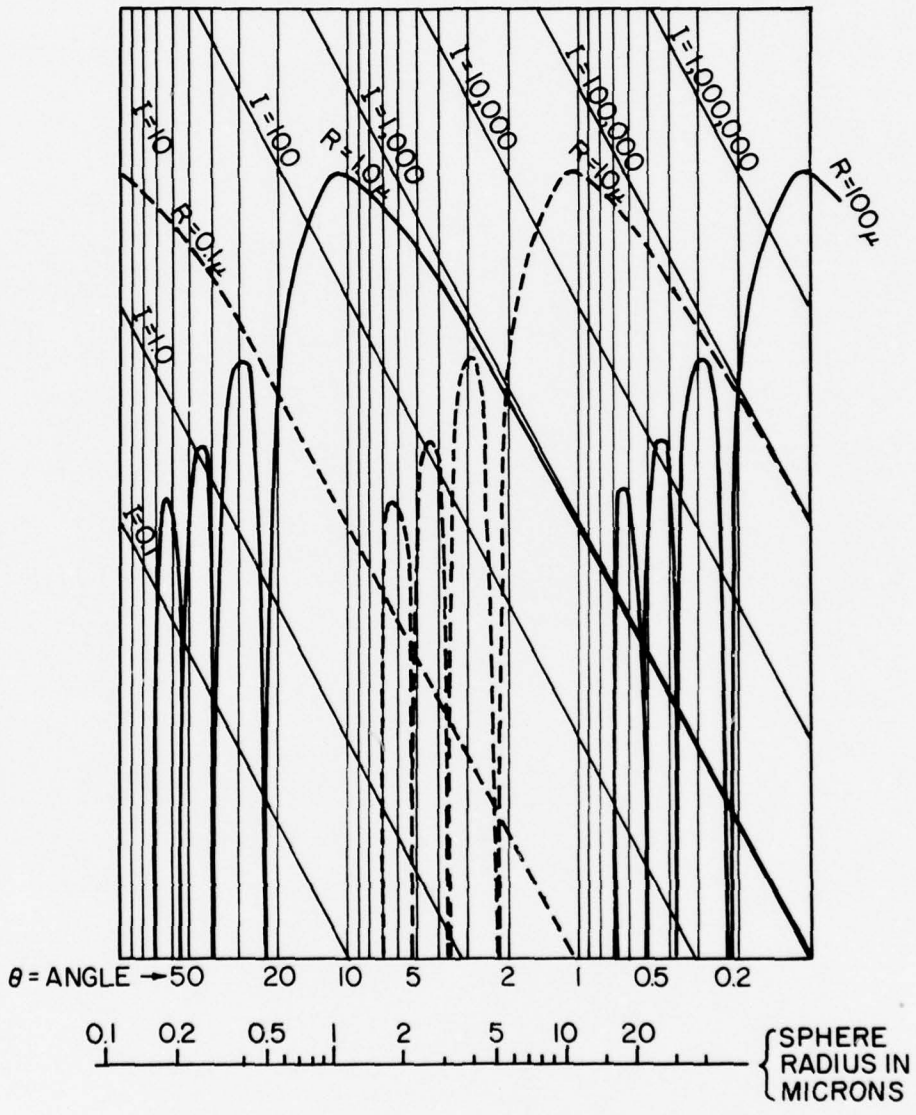

Figure 8. Schematic Plot of the $I\theta^2$ Curves for Spheres of Different Sizes (Sloan, 1954a).

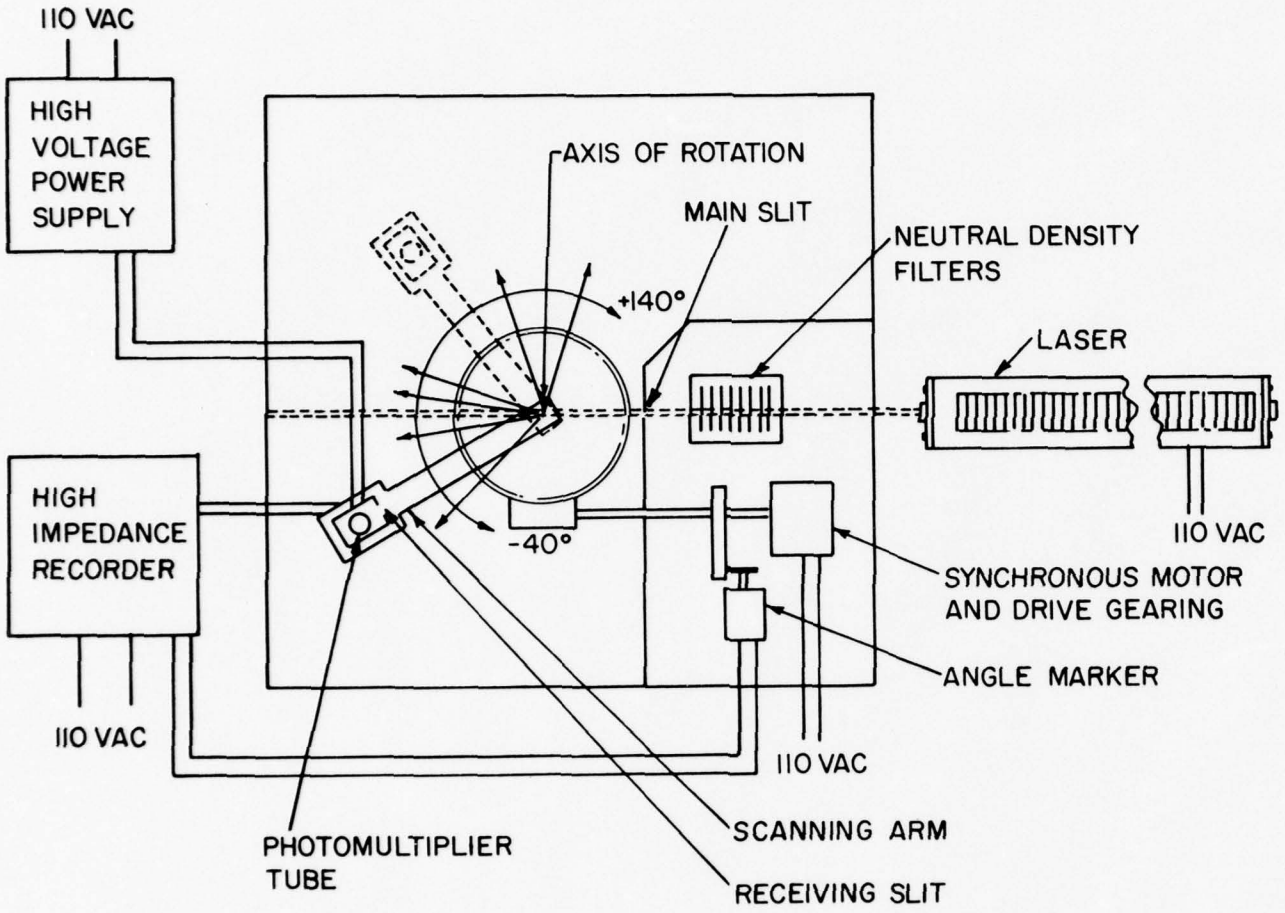

Figure 9. Schematic Diagram of the Goniophotometer.

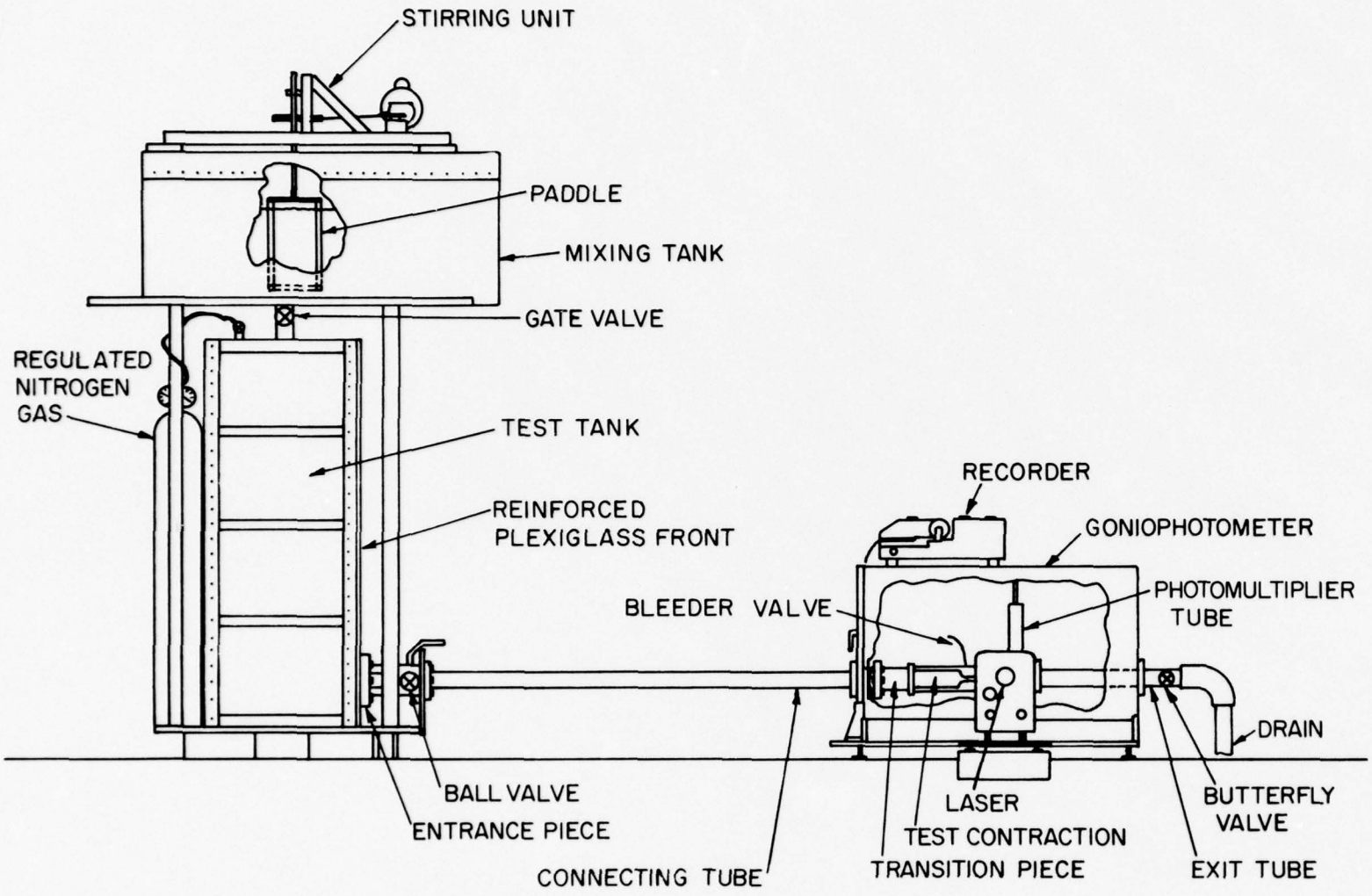

Figure 10. Schematic Diagram of the Test Set-up.

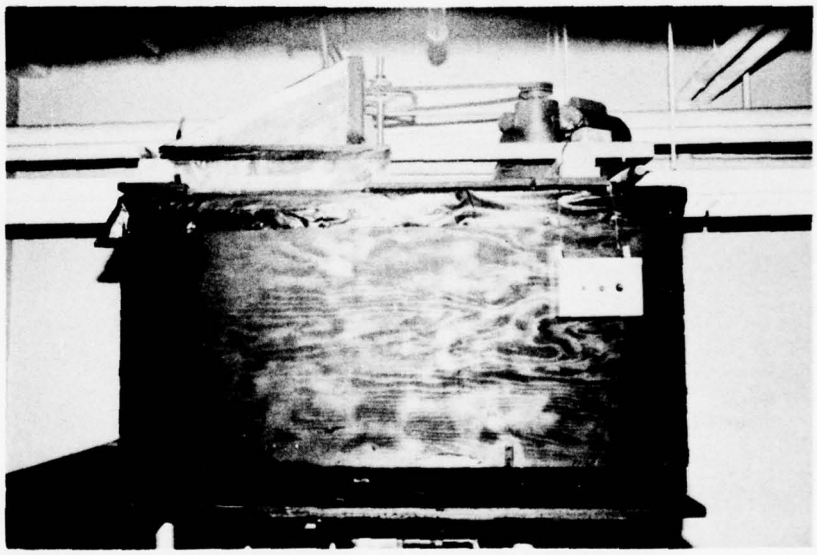

Figure 11. Photograph of the Mixing Tank and Stirring Unit.

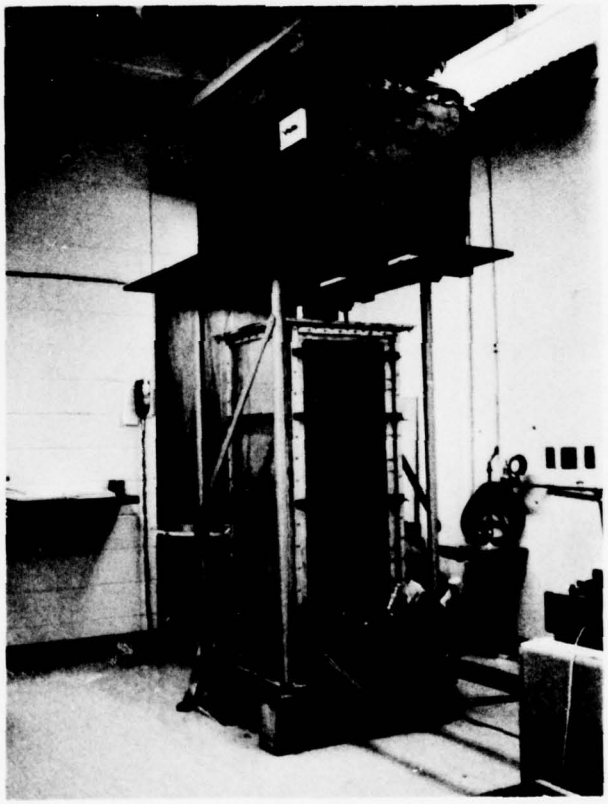

Figure 12. Photograph of the Test Tank Situated Below the Mixing Tank.

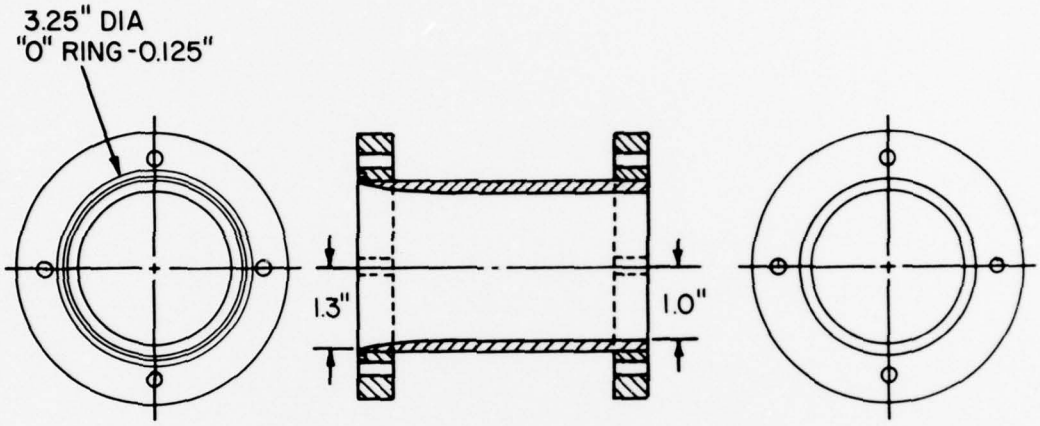

Figure 13. Diagram of the Smooth Streamlined Entrance Piece.

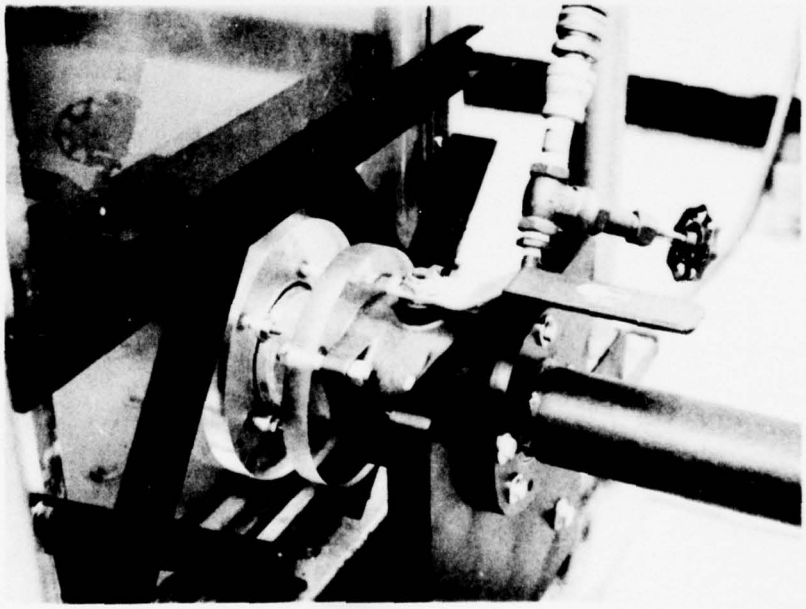

Figure 14. Photograph of the Smooth Entrance Piece Connected Between the Test Tank and the Ball Value (Handle in the Open Position).

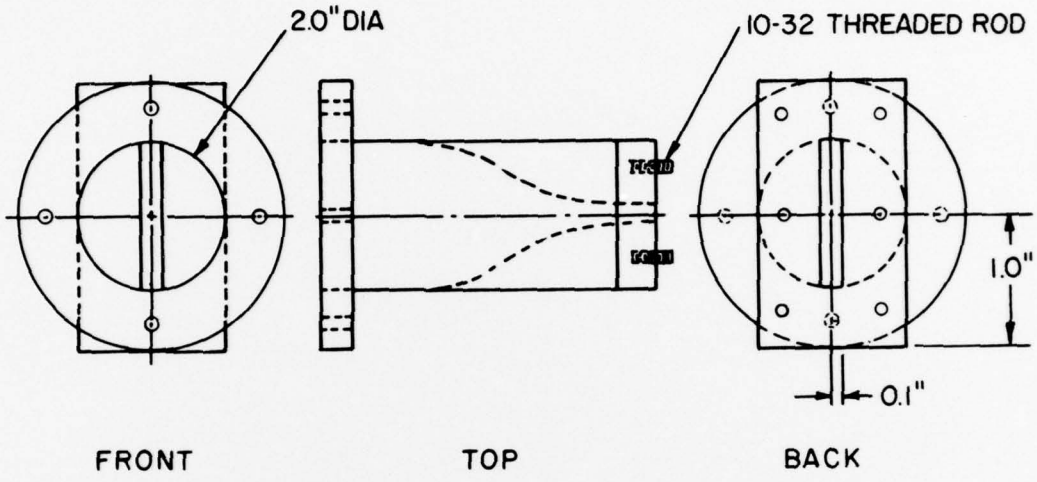

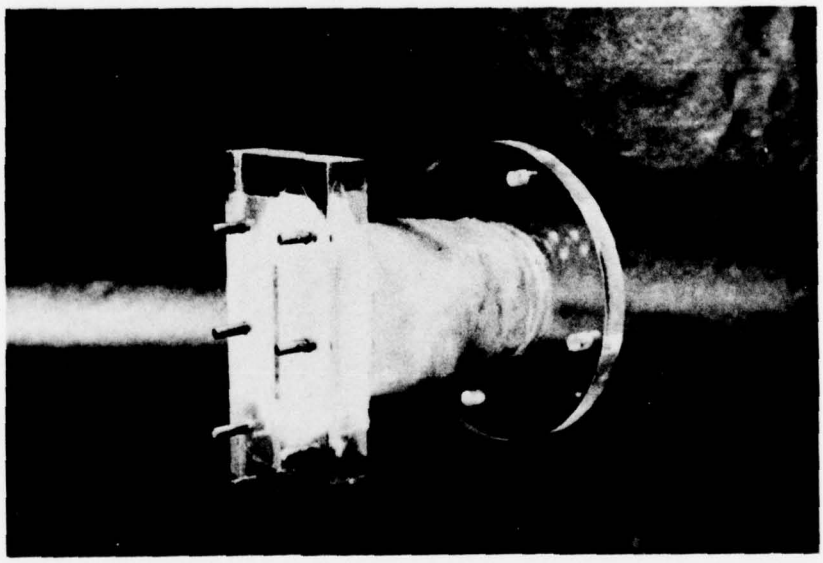

Figure 15. Diagram and Photograph of the Transition Piece.

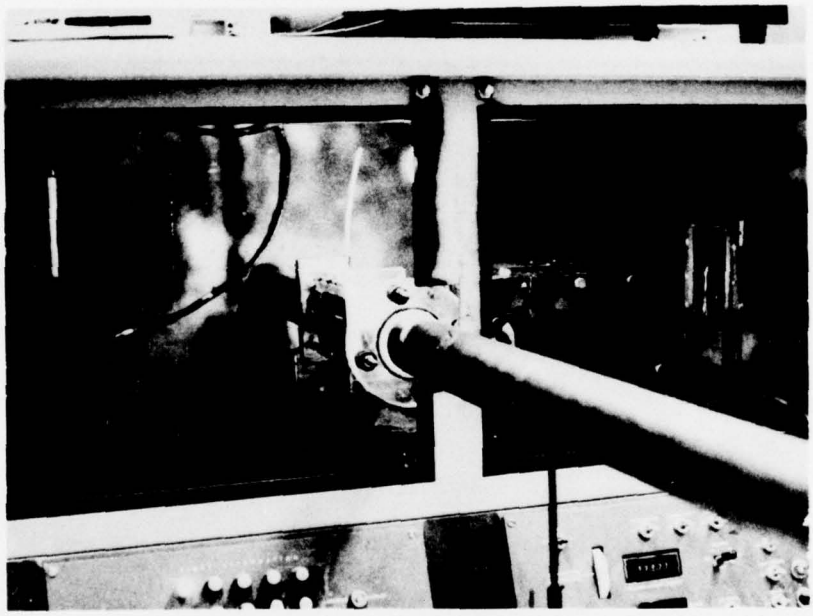

Figure 16. Photograph of the Test Contraction in Position Inside of the Goniophotometer.

Figure 17. Photograph of the Light Beam Striking the Centerline of the Test Contraction.

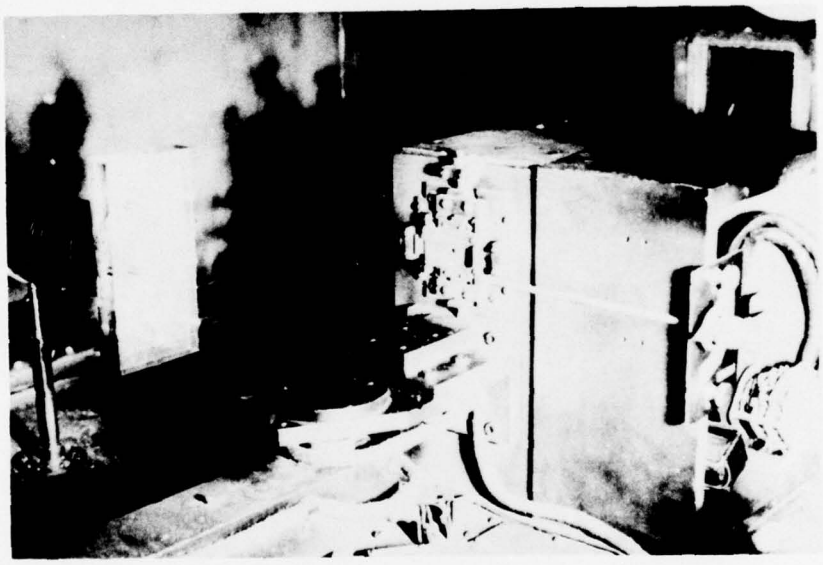

Figure 18. Photograph of the Adjustable Mounting Table.

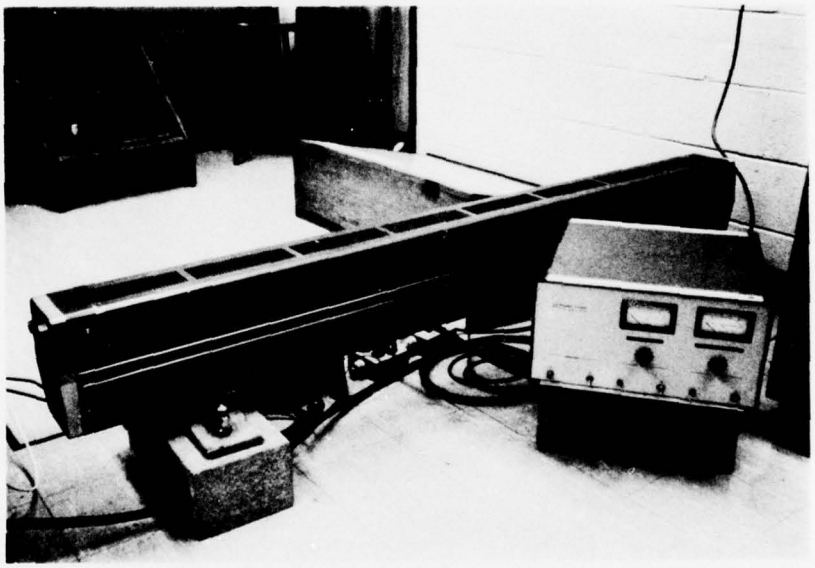

Figure 19. Photograph of the Spectra-Physics Model 125A (50 mw) He-Ne Gas Laser.

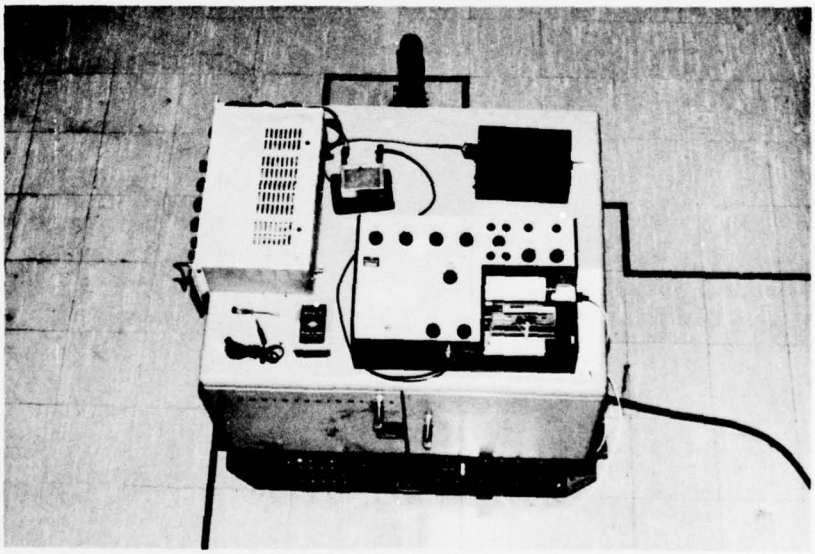

Figure 20. Photograph of the Recorder and Power Supply.

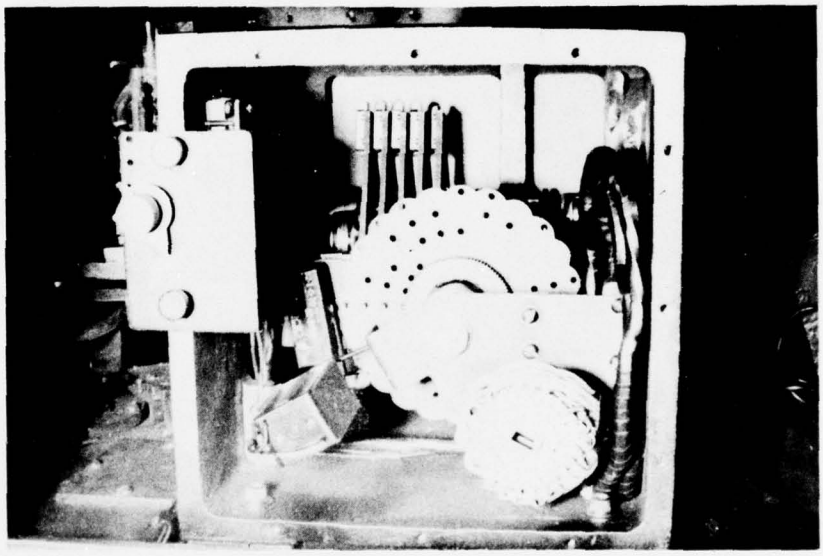

Figure 21. Photograph of the Neutral Density Filters Inside the Goniophotometer.

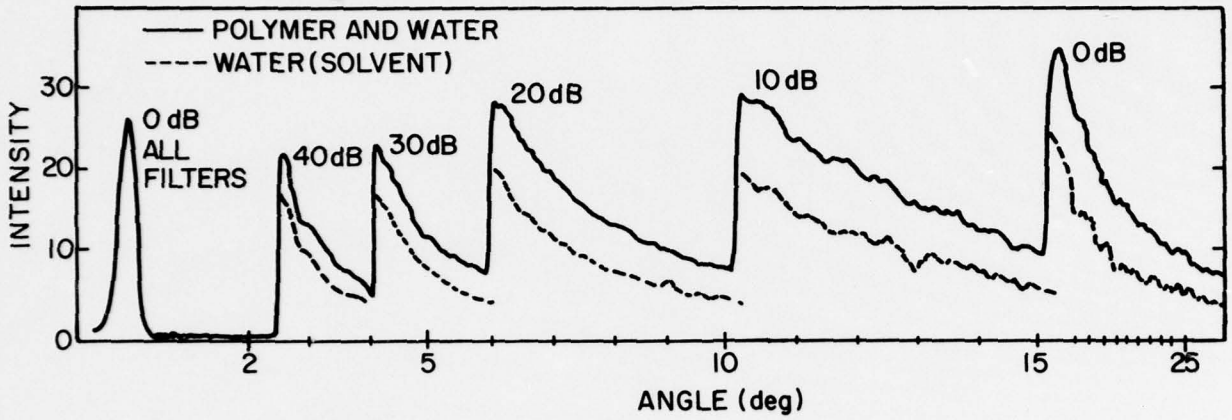

Figure 22. Typical Pattern of Light Scattering for a Still Polymer Sample, x = 0.60 in.

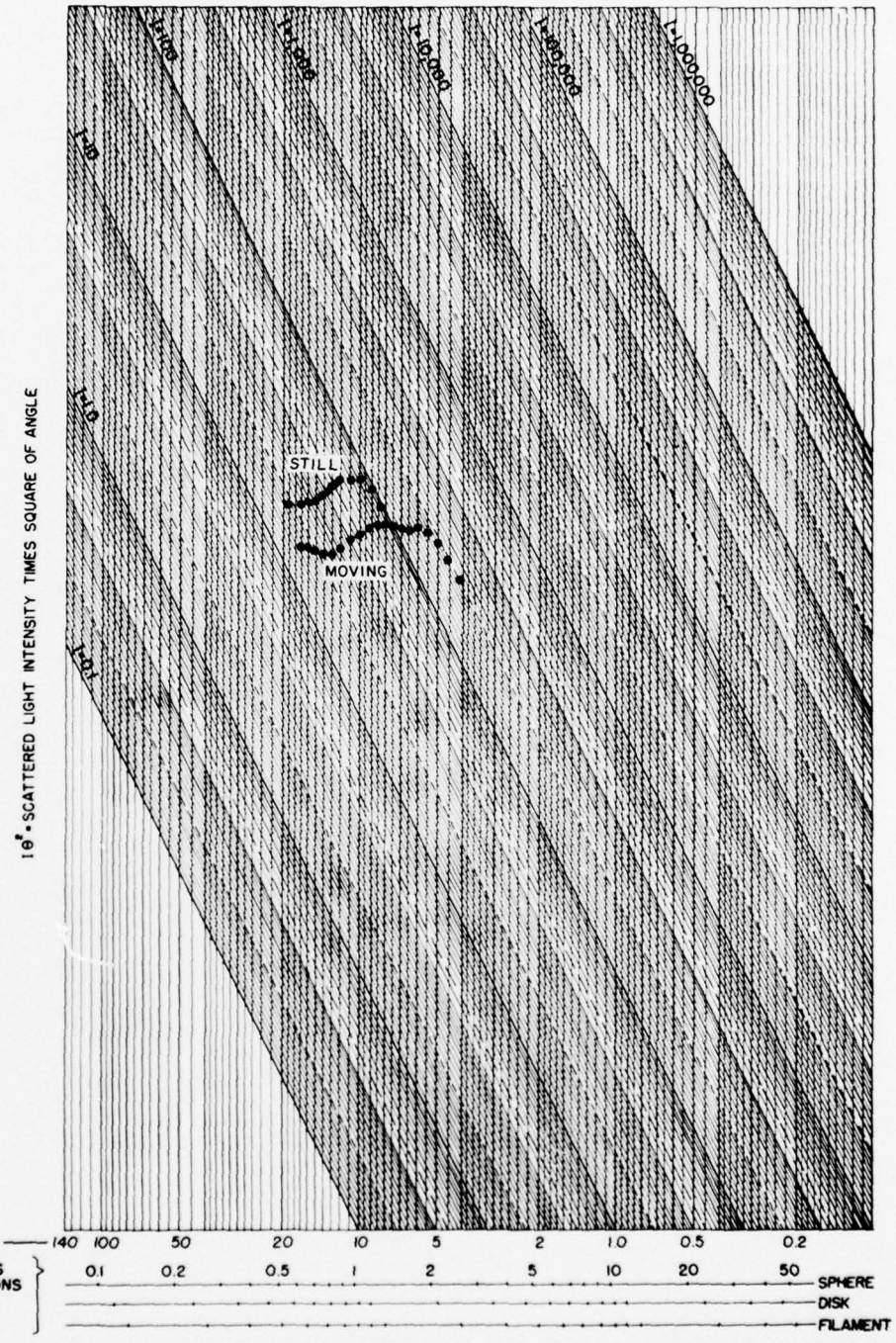

Figure 23. Scattered Light Intensity Times the Square of the Angle of Scatter Versus Angle of Scatter. Velocity = 19.2 fps., Concentration = 1600 ppmw., Position = 0.40.

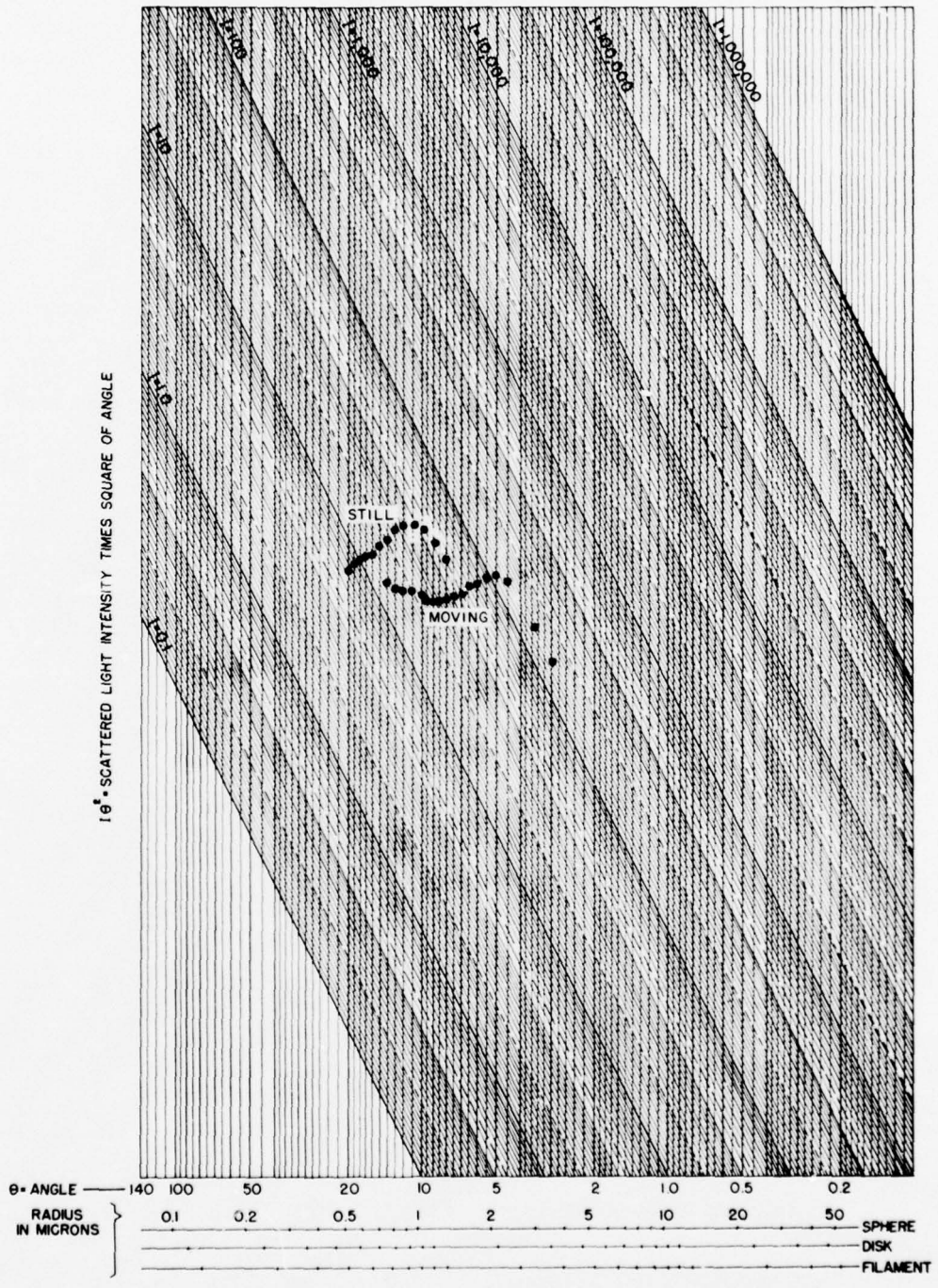

Figure 24. Scattered Light Intensity Times the Square of the Angle of Scatter Versus Angle of Scatter. Velocity = 19.2 fps., Concentration = 1600 ppmw., Position = 0.60.

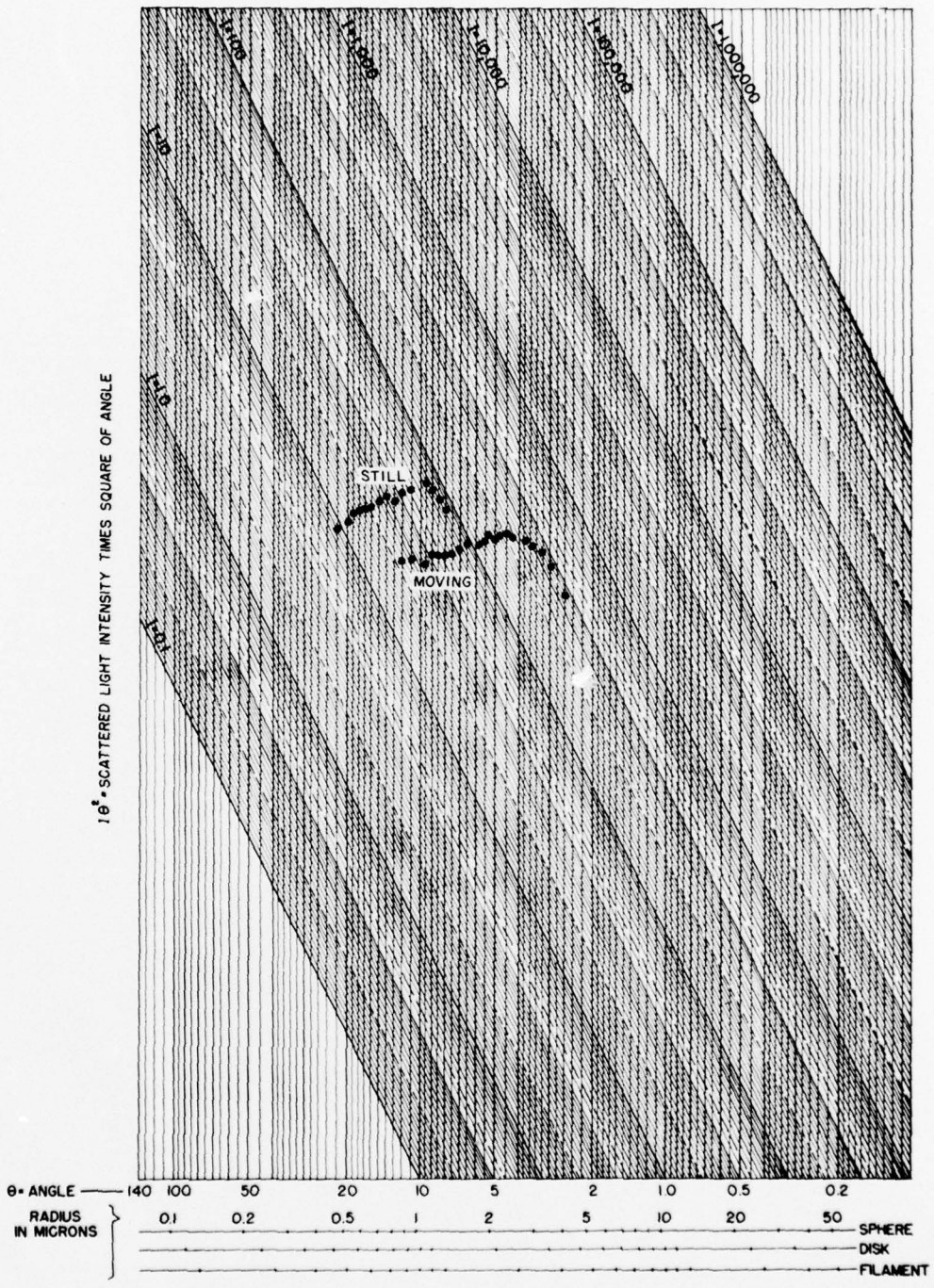

Figure 25. Scattered Light Intensity Times the Square of the Angle of Scatter Versus Angle of Scatter. Velocity = 19.2 fps., Concentration = 1600 ppmw., Position = 0.66.

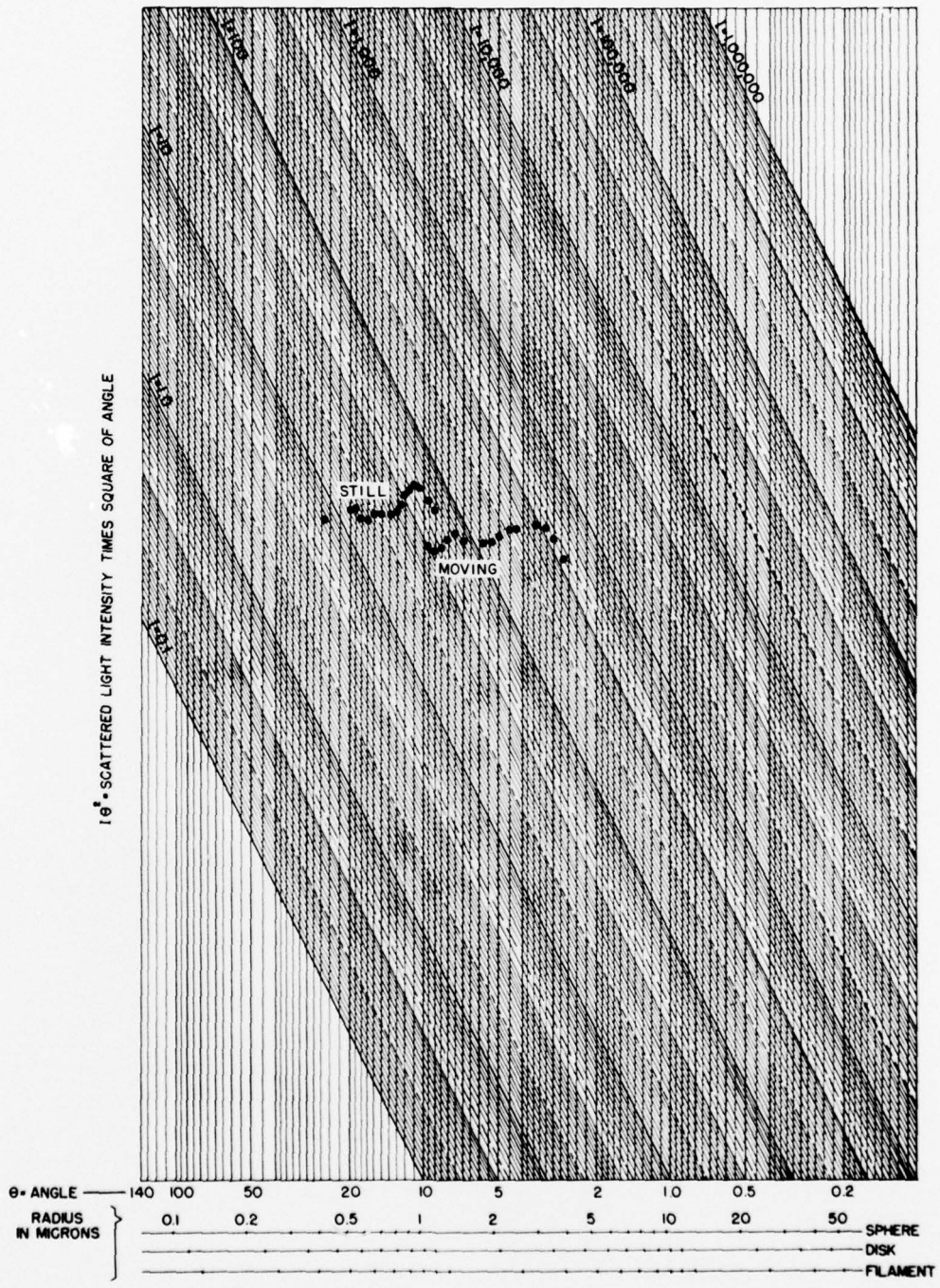

Figure 26. Scattered Light Intensity Times the Square of the Angle of Scatter Versus Angle of Scatter. Velocity = 19.2 fps. Concentration = 1600 ppmw., Position = 0.75.

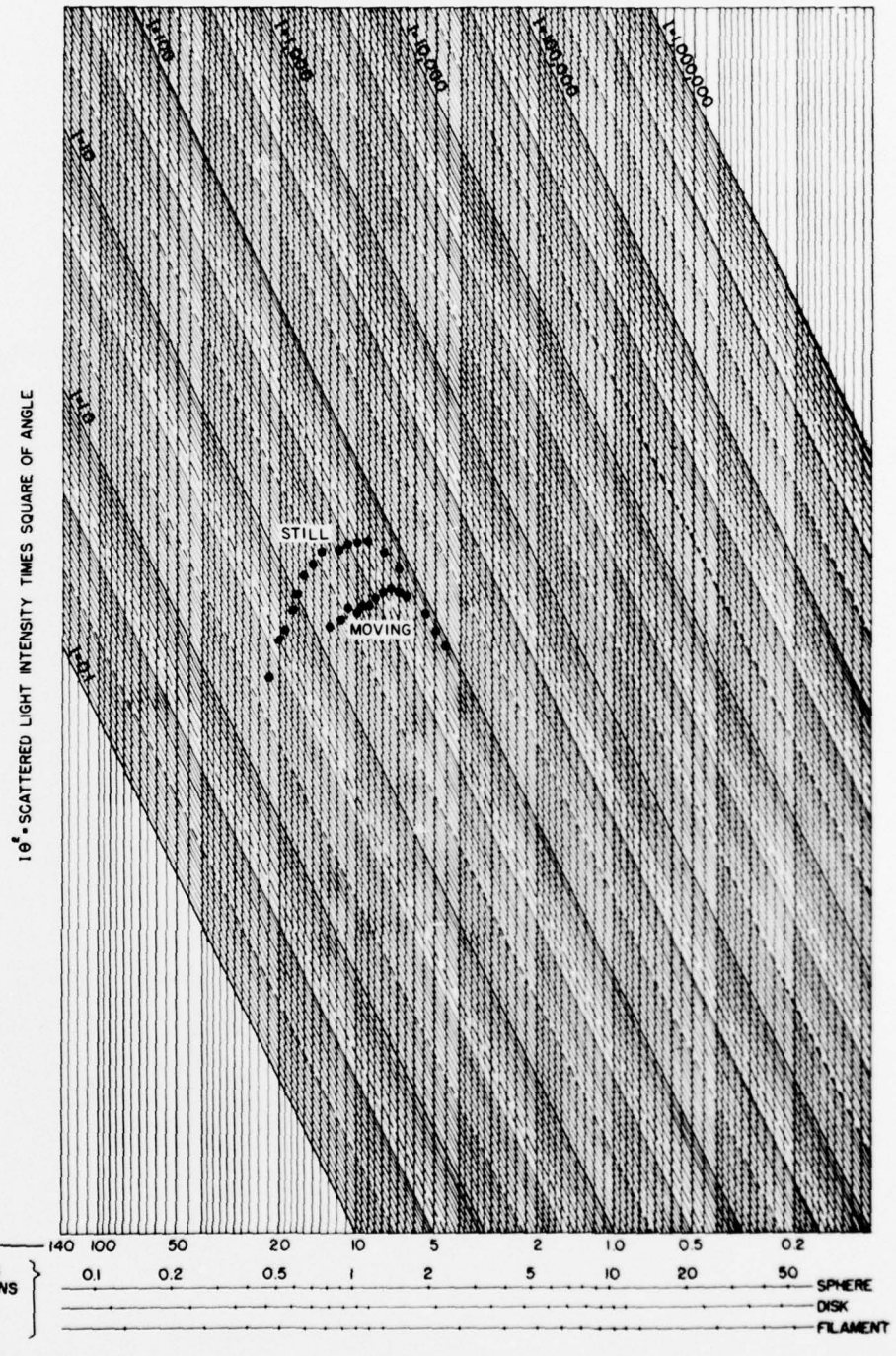

Figure 27. Scattered Light Intensity Times the Square of the Angle of Scatter Versus Angle of Scatter. Velocity = 19.2 fps., Concentration = 1600 ppmw., Position = 0.85.

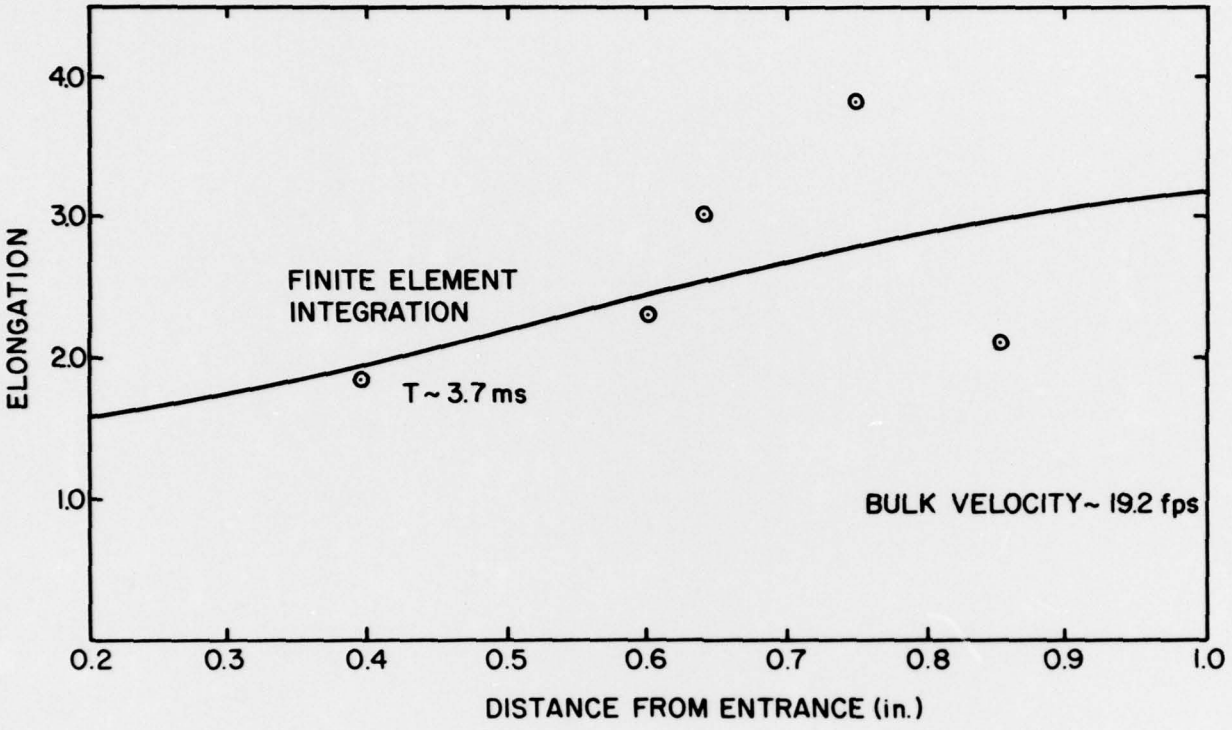

Figure 28. Elongation Versus Distance From the Test Contraction Entrance.